

1-1-1973

Magnetic feedback stabilization of a toroidal theta-pinch using helical fields

Randy Lee Hagenson
Iowa State University

Follow this and additional works at: <https://lib.dr.iastate.edu/rtd>

 Part of the [Engineering Commons](#)

Recommended Citation

Hagenson, Randy Lee, "Magnetic feedback stabilization of a toroidal theta-pinch using helical fields" (1973). *Retrospective Theses and Dissertations*. 18375.
<https://lib.dr.iastate.edu/rtd/18375>

This Thesis is brought to you for free and open access by the Iowa State University Capstones, Theses and Dissertations at Iowa State University Digital Repository. It has been accepted for inclusion in Retrospective Theses and Dissertations by an authorized administrator of Iowa State University Digital Repository. For more information, please contact digirep@iastate.edu.

Magnetic feedback stabilization of a
toroidal theta-pinch using helical fields

by

Randy Lee Hagenon

A Thesis Submitted to the
Graduate Faculty in Partial Fulfillment of
The Requirements for the Degree of
MASTER OF SCIENCE

Department: Chemical Engineering and Nuclear Engineering

Major: Nuclear Engineering

Signatures have been redacted for privacy

Iowa State University
Ames, Iowa

1973

TABLE OF CONTENTS

	<u>Page</u>
SYMBOLS	vi
ABSTRACT	viii
I. INTRODUCTION AND LITERATURE SURVEY	1
II. THEORETICAL DEVELOPMENT	4
A. Assumed Magnetic Field Configuration	4
B. Assumed Plasma Perturbations	9
C. Expansion Calculations	9
D. Growth Rates of Instabilities	43
III. COMPARISON OF EXPERIMENTAL AND THEORETICAL RESULTS	49
IV. DISCUSSION AND CONCLUSIONS	57
V. TOPICS FOR FURTHER STUDY	60
VI. LITERATURE CITED	61
VII. ACKNOWLEDGMENTS	62

LIST OF TABLES

	<u>Page</u>
Table 1. Summary of Scyllac experiments	50
Table 2. Summary of results from Scyllac	51

LIST OF FIGURES

	<u>Page</u>
Fig. 1. Ratio of maximum radial field to the plasma perturbation it produces versus ha for $\ell = 0$.	31
Fig. 2. Ratio of maximum radial field to the plasma perturbation it produces versus ha for $\ell = 1$.	32
Fig. 3. Ratio of maximum radial field to the plasma perturbation it produces versus ha for $\ell = 2$.	33
Fig. 4. Ratio of maximum radial field to the plasma perturbation it produces versus ha for $\ell = 3$.	34
Fig. 5. The quantity - $(R/a) \delta_0 \delta_1$ versus ha necessary for toroidal equilibrium.	35
Fig. 6. The quantity - $(R/a) \delta_\ell [\delta_{\ell+1}$ or $\delta_{\ell-1}]$ versus ha necessary for toroidal equilibrium.	36
Fig. 7. The quantity - $(R/a) \delta_\ell [\delta_{\ell+1}$ or $\delta_{\ell-1}]$ versus ha necessary for toroidal equilibrium.	37
Fig. 8. The quantity - $(R/a) \delta_\ell [\delta_{\ell+1}$ or $\delta_{\ell-1}]$ versus ha necessary for toroidal equilibrium.	38
Fig. 9. The quantity - $(R/a) B_r(\ell) B_r(\ell - 1) / B_0^2$ versus ha necessary for toroidal equilibrium.	39
Fig. 10. The quantity - $(R/a) B_r(\ell) [B_r(\ell - 1)$ or $B_r(\ell + 1)] / B_0^2$ versus ha necessary for toroidal equilibrium.	40
Fig. 11. The quantity - $(R/a) B_r(\ell) [B_r(\ell - 1)$ or $B_r(\ell + 1)] / B_0^2$ versus ha necessary for toroidal equilibrium.	41
Fig. 12. The quantity - $(R/a) B_r(\ell) [B_r(\ell - 1)$ or $B_r(\ell + 1)] / B_0^2$ versus ha necessary for toroidal equilibrium.	42
Fig. 13. Normalized growth rate versus ha for various β values and $\ell = 1$.	45
Fig. 14. Normalized growth rate versus ha for various β values and $\ell = 2$.	46
Fig. 15. Normalized growth rate versus ha for various β values and $\ell = 3$.	47
Fig. 16. The quantity - $(R/a) \delta_0 \delta_1$ versus β for experimental trials and theoretical solution.	54

- Fig. 17. The quantity $-\left(\frac{R}{a}\right) \frac{B(\ell = 1)B(\ell - 1 = 0)}{B_0^2}$ versus β for experimental trials and theoretical solution. 55
- Fig. 18. The quantity $\frac{B(\ell - 1 = 0)}{B_0 \delta_0}$ versus β for $ha = 0.19$. 56

SYMBOLS

a	- undisturbed plasma radius
B^{IN}	- magnetic field inside the plasma
B_0^{OUT}	- main confining field outside of plasma
B_r	- component of the magnetic field in the radial direction
B_z	- component of the magnetic field along the minor axis of the torus
B_θ	- component of the magnetic field about the minor axis
C_m	- Bessel function coefficient due to external helical windings
D_m	- Bessel function coefficient due to induced diamagnetic currents
F_m	- force applied by the helical fields
F_R	- toroidal force
f	- flux function due to toroidal curvature
$G_{\underline{l+1}}$	- a portion of the second-order flux function
h	- 2π divided by the wavelength of the helical field
I_m	- modified Bessel function of the first kind
K_m	- modified Bessel function of the second kind
l	- denotes the helical field being used
M_m	- sum of the applied and induced helical fields
m	- implies l or $\underline{l+1}$
p	- plasma pressure
R	- major radius of torus
R_l	- a portion of the applied plasma force function
r	- minor radius of torus
u	- angle variation of the helical fields
V_A	- Alfvén velocity

- V_g - growth rate of an unstable displacement of the plasma column
 $W_{\ell+1}$ - a portion of the applied helical fields
 x - magnetic scalar potential
 $Z_{\ell+1}$ - a portion of the applied helical fields
 z - minor axis of the torus
 β - ratio of plasma pressure to external magnetic field pressure
 γ - induced field arising from applied helical fields and toroidal curvature
 δ - plasma perturbation set equal to zero for plasma equilibrium
 δ_m - plasma perturbations arising from applied helical fields
 η - induced vertical field perpendicular to plane of torus
 θ - angle about the minor axis of the torus
 ξ - displacement of the plasma column
 ρ - plasma column density
 ψ - magnetic flux function

ABSTRACT

Ribe [7, 10] recently obtained equations describing necessary l and $l + 1$ helical fields which can compensate the natural toroidal drift present in the toroidal geometry. However, even though the numerical results are in good agreement with experimentation [8, 9, 12], the ordering used by Ribe [7, 10] is incorrect. Ribe [7, 10] assumes that $\delta \ll ha \cong 1$, but experimentation [9, 12] indicates that $ha \ll \delta \leq 1$ which is referred to as the new ordering. Using the new ordering expansion calculations are presented which produce the same final results as those given by the old ordering. Thus, the present expansion greatly extends the region over which the equations are applicable. Good agreement is found between theoretical results and experimental results from the Scyllac toroidal sector [9]. When the theoretical plasma equilibrium conditions are satisfied, the containment time is increased from 2.2 μsec (without helical fields) to nearly 12 μsec .

I. INTRODUCTION AND LITERATURE SURVEY

During the past decade and a half, linear theta-pinch experiments have demonstrated the production of hot, dense plasmas. The limitation on confinement time has been due to end losses and not to macro-instabilities.

In order to avoid this end loss problem, a toroidal theta-pinch can be used. However, it was shown by Greene, Johnson, and Weimer [4] that the plasma is shifted outward in the torus by an amount which increases with β , where the value of β is taken as

$$\beta = 1 - \frac{B^2}{B_0^2} .$$

Here, B is the magnetic field inside the plasma, and B_0 represents the main confining field outside the plasma. Thus, β has a maximum value of unity when B equals zero. This corresponds to a perfectly diamagnetic plasma from which the magnetic field is perfectly excluded.

The results given by Greene, Johnson, and Weimer [4] indicate that the toroidal shift becomes very large for β greater than about 0.082. Since the theta-pinch uses a β of about 0.9, the plasma is immediately driven to the wall of the toroidal device.

References [3, 6, 11] then studied possible ways of obtaining a toroidal equilibrium. The conclusions that were drawn indicate that equilibrium could be produced using additional helical windings. However, the specific form of the necessary fields was still not known.

A toroidal equilibrium was then demonstrated by Blank, Grad, and Weitzner [1] for a high beta plasma having a sharp boundary. The use

of simple helical windings produced the necessary fields for plasma equilibrium. Knowing the general form of the necessary helical fields, numerical results for design experiments were then needed.

Ribe [7, 10] produced equations describing necessary l and $l \pm 1$ helical fields which can compensate the natural toroidal drift present in the toroidal geometry. The necessary numerical results were also given for use in designing a theta-pinch. However, even though the numerical results were in good agreement with experimentation [8, 9, 12], many of the assumptions used by Ribe [7, 10] in deriving the design equations were incorrect.

In order to solve the stabilization problem, it is necessary to assume the magnitudes of the l and $l \pm 1$ helical fields that must be applied in order to cancel the toroidal drift. The magnitudes of the plasma perturbations, given by δ , caused by the helical fields must also be assumed. Ribe [7, 10] assumes that $\delta \ll ha \cong 1$, which will be referred to as the old ordering. However, various experiments [9, 12] indicate that δ may become rather large when $ha = 0.15$, where $2\pi/h$ is the pitch of the helical field, and a is the undisturbed plasma radius. Hence, the ordering should be changed to $ha \ll \delta \leq 1$, which will be referred to as the new ordering.

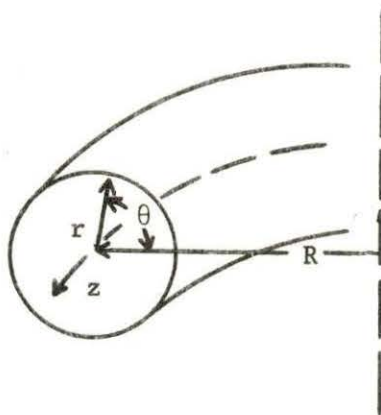
This led Weitzner [13] to devise a new theory using the new ordering. The solutions found correspond in the appropriate limit to those given by Ribe [7, 10] except for the growth rate of the plasma column caused by the helical fields. The new ordering predicts a growth rate about 50% less than that predicted by the old ordering. However, Freidberg [2] has shown that the theory given by Weitzner [13]

can be improved upon by including higher-order terms using numerical techniques. When this is done, the growth rates predicted by the new ordering and the old ordering are in good agreement.

The theory using the new ordering produces results only in the limit as h_a approaches zero. Whereas, the results given by Ribe [7, 10] are in terms of the applied fields, which make it possible to design a theta-pinch reactor.

This thesis intends to use the new ordering in order to produce results of the same form as given by Ribe [7, 10].

The following coordinate system will be used:



In the toroidal system R is taken as the major radius, and r is taken as the minor radius. The minor axis of the torus is denoted by z , and the angle about z is given by θ .

II. THEORETICAL DEVELOPMENT

A. Assumed Magnetic Field Configuration

The magnetic field is assumed to be given by

$$B = B^{(0)} \hat{e}_z \left(1 - \frac{r}{R} \cos \theta + \frac{r^2}{R^2} \cos^2 \theta\right) + B^{(0)} \nabla x \quad (1)$$

where the scalar potential x includes

$$\begin{aligned} x = & \frac{1}{h} M_\ell(hr) \sin(\ell\theta - hz) \\ & + \frac{1}{h} M_{\ell-1}(hr) \sin[(\ell - 1)\theta - hz] \\ & + \frac{1}{h} M_{\ell+1}(hr) \sin[(\ell + 1)\theta - hz] \\ & + \left(\frac{r}{h} + \frac{y}{h^2 r}\right) \sin \theta . \end{aligned} \quad (2)$$

The main field $B^{(0)}$ is distorted by the toroidal curvature which is indicated by the terms

$$- \frac{r}{R} \cos \theta + \frac{r^2}{R^2} \cos^2 \theta$$

where r represents the plasma radius, and R denotes the major toroidal radius. Latest experiments on the Scyllac theta-pinch [9] indicate that a toroidal system will use $r = 1.0$ centimeter and $R = 800$ centimeters. This results in $r/R = 1.25 \times 10^{-3}$ and implies that the magnitude of this term can be taken as third-order. The term $r^2/R^2 \cos^2 \theta$ can then be taken as sixth-order and is not significant in the theoretical derivation.

The helical fields are described by Bessel functions of argument ha . The term $2\pi/h$ is the pitch of the helical field, and a is the undisturbed plasma radius.

The modified Bessel function

$$M_{\ell}(hr) = [C_{\ell} I_{\ell}(hr) + D_{\ell} K_{\ell}(hr)] \quad (3)$$

represents the ℓ -order helical field that would be applied in order to cancel the toroidal distortion. The quantity C_{ℓ} is given by the external helical windings, and the D_{ℓ} term is due to induced currents in the plasma configuration. Scyllac [9] experiments use an $\ell = 1$ magnetic field that has an approximate magnitude of

$$\frac{M_{\ell}}{B(0)} = 0.07 - 0.08.$$

Thus, the ℓ -order field will be taken as a first-order quantity.

The second-order quantity

$$M_{\ell+1}(hr) = [C_{\ell+1} I_{\ell+1}(hr) + D_{\ell+1} K_{\ell+1}(hr)] \quad (4)$$

represents a smaller applied helical field that is necessary to fully cancel the toroidal drift.

The second-order $\sin \theta$ terms represent quantities that will be induced by the helical windings. These terms consist of $\eta r \sin \theta$ which represents a vertical field perpendicular to the plane of the torus. This field arises from external wires carrying currents on both sides of the plasma. Other terms including $\gamma/h^2 r \sin \theta$ will also be present due to toroidal curvature.

In the following ordering procedure ha is taken as a first-order quantity.

It is seen that

$$\nabla x = \frac{\partial x}{\partial r} \bar{e}_r + \frac{1}{r} \frac{\partial x}{\partial \theta} \bar{e}_\theta + \frac{\partial x}{\partial z} \bar{e}_z . \quad (5)$$

The following ordering will be used for all l and $l \pm 1$ except the case $M_{l-1} = M_0$ which must be treated separately. The number in parenthesis represents the order. The equations can be written as

$$B_\theta^{(1)} = \frac{B^{(0)}_l}{hr} M_l \cos u, \quad (6)$$

$$B_r^{(1)} = B^{(0)} M'_l \sin u, \quad (7)$$

$$B_z^{(1)} = 0, \quad (8)$$

$$B_\theta^{(2)} = \frac{B^{(0)}_{(l+1)}}{hr} M_{l+1} \cos(u + \theta) + \frac{B^{(0)}_{(l-1)}}{hr} M_{l-1} \cos(u - \theta) + B^{(0)} \left(\eta + \frac{\gamma}{h^2 r^2} \right) \cos \theta, \quad (9)$$

$$B_r^{(2)} = B^{(0)} M'_{l+1} \sin(u + \theta) + B^{(0)} M'_{l-1} \sin(u - \theta) + B^{(0)} \left(\eta - \frac{\gamma}{h^2 r^2} \right) \sin \theta, \quad (10)$$

$$B_z^{(2)} = - B^{(0)} M_l \cos u, \quad (11)$$

$$B_z^{(3)} = - B^{(0)} M_{l+1} \cos(u + \theta) - B^{(0)} M_{l-1} \cos(u - \theta) - \frac{B^{(0)}_r}{R} \cos \theta \quad (12)$$

where

$$u = l\theta - hz,$$

and

$$M_{l-1} \neq M_0 .$$

It is seen that the ℓ and $\ell \pm 1$ B_z fields can be considered as higher-order because ha is taken as first-order.

One can show that the B_r and B_θ terms should be of the same order. For small ha the small argument approximations can be used for the Bessel functions given by

$$I_m = \frac{1}{m!} \left(\frac{ha}{2}\right)^m, \quad (13)$$

$$I'_m = \frac{1}{2} \frac{1}{(m-1)!} \left(\frac{ha}{2}\right)^{m-1}, \quad (14)$$

$$K_m = \frac{1}{2} (m-1)! \left(\frac{2}{ha}\right)^m, \quad (15)$$

$$K'_m = -\frac{1}{4} m! \left(\frac{2}{ha}\right)^{m+1}, \quad (16)$$

where

$$m = 1, 2, 3, 4, \dots$$

It is noted that the approximations for the modified Bessel functions are accurate to within 1% of the true I_m and I'_m for values of ha as large as 0.25. However, the values for K_m and K'_m given above may be 6-7% off for ha as large as 0.25.

Using Eq. (3) and noting that inside the plasma column D_ℓ must be zero because K_ℓ approaches infinity at $r = 0$, one obtains

$$M_\ell^{IN} = C_\ell^{IN} I_\ell,$$

$$M_\ell'^{IN} = C_\ell^{IN} I_\ell',$$

where the superscript "IN" implies that the expression describes the inside of the plasma column.

Using the small argument approximations, one obtains

$$\frac{\frac{\ell}{hr} M_{\ell}^{IN}}{M_{\ell}^{\prime IN}} = \frac{\frac{\ell}{hr} I_{\ell}}{I_{\ell}^{\prime}} = 1.$$

Thus, on the inside of the plasma column $B_r^{(1)}$ and $B_{\theta}^{(1)}$ are approximately equal for small ha . The same arguments indicate that on the outside of the plasma column $B_r^{(1)}$ and $B_{\theta}^{(1)}$ are not equal, but they are definitely of the same order. It can also be shown by the above procedure that $B_r^{(2)}$ and $B_{\theta}^{(2)}$ are of the same order of magnitude.

In the special case where $\ell = 1$ and $\ell - 1 = 0$, the ordering must be changed. Taking $M_{\ell-1} = M_0$ and $M_{\ell-1}^{\prime} = M_0^{\prime}$ only on the inside of the plasma column gives

$$\frac{M_0}{M_0^{\prime}} = \frac{I_0}{I_0^{\prime}} = \frac{2}{ha}.$$

The B_z field for the M_0 case is actually an order of magnitude larger than the B_r field on the inside of the plasma. Here M_0 is taken as first-order, and M_0^{\prime} is left as a second-order quantity. Only the ordering of one term must be changed in Eqs. (6-12). The term

$$- B^{(0)} M_{\ell-1} \cos(u - \theta)$$

must be moved from third- to first-order when $M_{\ell-1} = M_0$. In this case Eq. (8) must be changed to

$$B_z^{(1)} = - B^{(0)} M_0 \cos hz, \quad (17)$$

and Eq. (12) must be changed to

$$B_z^{(3)} = -B^{(0)} M_2 \cos(u + \theta) - \frac{B^{(0)} r}{R} \cos \theta \quad (18)$$

for $M_{\ell-1} = M_0$.

B. Assumed Plasma Perturbations

The equation of a field line expanded about a particular radius $r = a$ is assumed to be

$$r(z, \theta) = a[1 + \delta_\ell^{(0)} \cos u + \delta^{(1)} \cos \theta + \delta_{\ell+1}^{(1)} \cos(u + \theta) + \delta_{\ell-1}^{(1)} \cos(u - \theta)]. \quad (19)$$

The perturbations given by $\delta_\ell \cos u$ and $\delta_{\ell+1} \cos(u \pm \theta)$ are derived from the applied helical windings. The expression $\delta \cos \theta$ results from the nonhomogeneous toroidal magnetic field and gives rise to the toroidal drift. This $\delta \cos \theta$ term is taken as first-order. In order to have plasma stabilization, the δ term must be zero.

Experiments on the Scyllac sector [9] have shown that $\delta_1 \cos u$ may be approximately 1.0 for most experiments. This term is then taken as zero-order. The perturbation given by $\delta_0 = \delta_{\ell-1}$ is about 0.2 in most experiments and is taken as first-order.

C. Expansion Calculations

One begins with

$$\bar{B} \cdot \bar{\nabla} \psi = 0. \quad (20)$$

Previous work done on magnetic field structures by Morozov and Solov'ev [5] indicates that the magnetic flux surfaces obey

$$\psi(r, \theta) = \frac{1}{2} hr^2 B^{(0)} - B^{(0)} r \sum_{n=1}^{\infty} M'_\ell(nhr) \cos n(\ell\theta - hz) = \text{constant} \quad (21)$$

where

$$\ell = 1, 2, 3, \dots$$

Equation (21) is valid only for a linear theta-pinch with helical windings. It will be seen that an additional term will arise in the equation describing the magnetic surfaces when a toroidal curvature is present.

The first-order flux function can be taken to be

$$\psi^{(1)} = \frac{1}{2} hr^2 - rM'_\ell \cos u \quad (22)$$

from Eq. (21). The term $\frac{1}{2} hr^2$ is due to the main confining field $B^{(0)}$, and $-rM'_\ell \cos u$ arises from the applied helical windings.

Expanding Eq. (20) produces

$$\begin{aligned} 0 = & [B^{(0)} + B_z^{(1)} + B_z^{(2)} + B_z^{(3)}] \left[\frac{\partial}{\partial z} \psi^{(1)} + \frac{\partial}{\partial z} \psi^{(2)} + \frac{\partial}{\partial z} \psi^{(3)} \right] \\ & + [B_r^{(1)} + B_r^{(2)} + B_r^{(3)}] \left[\frac{\partial}{\partial r} \psi^{(1)} + \frac{\partial}{\partial r} \psi^{(2)} + \frac{\partial}{\partial r} \psi^{(3)} \right] \\ & + [B_\theta^{(1)} + B_\theta^{(2)} + B_\theta^{(3)}] \left[\frac{1}{r} \frac{\partial}{\partial \theta} \psi^{(1)} + \frac{1}{r} \frac{\partial}{\partial \theta} \psi^{(2)} + \frac{1}{r} \frac{\partial}{\partial \theta} \psi^{(3)} \right]. \end{aligned} \quad (23)$$

It should be noticed that $B^{(0)} \frac{\partial}{\partial z} \psi^{(1)}$ is a second-order quantity because h is considered first-order, while $B^{(0)} \frac{\partial}{\partial r} \psi^{(1)}$ and $\frac{B^{(0)}}{r} \frac{\partial}{\partial \theta} \psi^{(1)}$ are both first-order quantities.

There are no first-order terms in Eq. (23). The second-order terms require that

$$0 = B^{(0)} \frac{\partial}{\partial z} \psi^{(1)} + B_r^{(1)} \frac{\partial}{\partial r} \psi^{(1)} + \frac{B_\theta^{(1)}}{r} \frac{\partial}{\partial \theta} \psi^{(1)}, \quad (24)$$

and the third-order terms also require that

$$0 = B_z^{(1)} \frac{\partial}{\partial z} \psi^{(1)} + B^{(0)} \frac{\partial}{\partial z} \psi^{(2)} + B_r^{(1)} \frac{\partial}{\partial r} \psi^{(2)} \\ + B_r^{(2)} \frac{\partial}{\partial r} \psi^{(1)} + \frac{B_\theta^{(1)}}{r} \frac{\partial}{\partial \theta} \psi^{(2)} + \frac{B_\theta^{(2)}}{r} \frac{\partial}{\partial \theta} \psi^{(1)}. \quad (25)$$

Checking to see if $\psi^{(1)}$ satisfies Eq. (24) gives

$$B^{(0)} [-hrM'_\ell \sin u] + B^{(0)} [M'_\ell \sin u] [hr - M'_\ell \cos u - hrM''_\ell \cos u] \\ + \frac{\ell B^{(0)}}{hr} M_\ell \cos u [\ell M'_\ell \sin u] = 0. \quad (26)$$

Bessel's equation

$$M''_\ell = -\frac{M'_\ell}{hr} + \left(1 + \frac{\ell^2}{h^2 r^2}\right) M_\ell \quad (27)$$

is then used to substitute for M''_ℓ in Eq. (26). The approximation that

$$M''_\ell \simeq -\frac{M'_\ell}{hr} + \frac{\ell^2}{h^2 r^2} M_\ell \quad (28)$$

must then be used. This is a good approximation since $\ell^2/h^2 r^2$ is 50 to 100 times larger than 1. Equation (26) is then satisfied when Eq. (28) is substituted for M''_ℓ .

Substituting into Eq. (25) for the more general case where $M_{\ell-1} \neq M_0$ gives

$$\begin{aligned}
& B^{(0)} \frac{\partial}{\partial z} \psi^{(2)} + [B^{(0)} M'_\ell \sin u] \left[\frac{\partial}{\partial r} \psi^{(2)} \right] \\
& + \left[\frac{\ell B^{(0)}}{hr} M_\ell \cos u \right] \left[\frac{1}{r} \frac{\partial}{\partial \theta} \psi^{(2)} \right] + B^{(0)} \left[M'_{\ell \pm 1} \sin(u \pm \theta) \right. \\
& + \left. \left(\eta - \frac{\gamma}{h^2 r^2} \right) \sin \theta \right] [hr - M'_\ell \cos u - hr M''_\ell \cos u] \\
& + B^{(0)} \left[\frac{(\ell \pm 1)}{hr} M_{\ell \pm 1} \cos(u \pm \theta) \right. \\
& + \left. \left(\eta + \frac{\gamma}{h^2 r^2} \right) \cos \theta \right] [\ell M'_\ell \sin u] = 0. \tag{29}
\end{aligned}$$

The notation $M_{\ell \pm 1}$ implies that

$$M_{\ell \pm 1} \cos(u \pm \theta) = M_{\ell-1} \cos(u - \theta) + M_{\ell+1} \cos(u + \theta). \tag{30}$$

It is now assumed that

$$\psi^{(2)} = f(r) \cos \theta + G_{\ell \pm 1} \cos(u \pm \theta) \tag{31}$$

where $f(r) \cos \theta$ results from the toroidal curvature of the field, and $G_{\ell \pm 1} \cos(u \pm \theta)$ may result from the $\ell \pm 1$ helical field, or the interaction of the ℓ helical field with $f(r) \cos \theta$.

Substituting $\psi^{(2)}$ into Eq. (29) gives

$$\begin{aligned}
0 = & B^{(0)} h G_{\ell \pm 1} \sin(u \pm \theta) + B^{(0)} M'_\ell \sin u [f'(r) \cos \theta + G'_{\ell \pm 1} \cos(u \pm \theta)] \\
& + \frac{\ell B^{(0)}}{hr^2} M_\ell \cos u [-f(r) \sin \theta - (\ell \pm 1) G_{\ell \pm 1} \sin(u \pm \theta)] \\
& + B^{(0)} \left[M'_{\ell \pm 1} \sin(u \pm \theta) + \left(\eta - \frac{\gamma}{h^2 r^2} \right) \sin \theta \right] \left[hr - \frac{\ell^2}{hr} M_\ell \cos u \right] \\
& + B^{(0)} \left[\frac{(\ell \pm 1)}{hr} M_{\ell \pm 1} \cos(u \pm \theta) + \left(\eta + \frac{\gamma}{h^2 r^2} \right) \cos \theta \right] [\ell M'_\ell \sin u]. \tag{32}
\end{aligned}$$

The $\sin(u \pm \theta)$ terms require that

$$G_{\underline{l+1}} \sin(u \pm \theta) = \left[-rM'_{\underline{l+1}} - \frac{M'_l f'}{2h} \pm \frac{l f M_l}{2h^2 r^2} \right] \sin(u \pm \theta), \quad (33)$$

which gives

$$\psi^{(2)} = f(r) \cos \theta + \left[-rM'_{\underline{l+1}} - \frac{M'_l f'}{2h} \pm \frac{l f M_l}{2h^2 r^2} \right] \cos(u \pm \theta). \quad (34)$$

It is noted that the terms

$$-\frac{l^2}{hr} M_l \left(\eta - \frac{\gamma}{h^2 r^2} \right) \sin \theta \cos u + l M'_l \left(\eta + \frac{\gamma}{h^2 r^2} \right) \cos \theta \sin u \quad (35)$$

also produce $\sin(u \pm \theta)$ terms. However, because of the following approximation, these terms are considered small.

Experiments on the Scyllac five-meter toroidal sector have shown that the toroidal drift is effectively cancelled using $B_{\ell=1}/B_0 \approx 0.08$. Larger helical fields were tried, but the containment times were shorter. Taking the square of the $\ell = 1$ field gives

$$[B_{\ell=1}]^2 = [0.08 \cos(\theta - hz)]^2 = 0.0032[1 + \cos 2(\theta - hz)].$$

Thus, the square of this first-order quantity has produced a third-order term instead of the expected second-order result. The consequences of this can be shown by first obtaining the relation between $f(r)$ and $(\eta - \gamma/h^2 r^2)$ from Eq. (32) by equating $\sin \theta$ terms which gives

$$\begin{aligned} \left(\eta - \frac{\gamma}{h^2 r^2} \right) \sin \theta = & \frac{M'_l G'_{\underline{l+1}} \sin(\pm \theta)}{2hr} + \frac{l(l \pm 1) M_l G_{\underline{l+1}} \sin(\pm \theta)}{2h^2 r^2} \\ & + \frac{l^2 M'_{\underline{l+1}} M_l \sin(\pm \theta)}{2h^2 r^2} + \frac{(l \pm 1) l M_{\underline{l+1}} M'_l \sin(\pm \theta)}{2h^2 r^2}. \quad (36) \end{aligned}$$

Substituting Eq. (36) into the first term of Eq. (35) gives

$$\begin{aligned}
-\frac{\ell^2}{2hr} M_\ell \left(\eta - \frac{\gamma}{h^2 r^2} \right) \sin(u \pm \theta) = & -\frac{\ell^2}{2hr} M_\ell \left[\frac{M'_\ell G'_{\ell+1}}{2hr} + \frac{\ell(\ell \pm 1) M_\ell G_{\ell+1}}{2h^2 r^3} \right. \\
& \left. + \frac{\ell^2 M'_{\ell+1} M_\ell}{2h^2 r^2} + \frac{(\ell \pm 1) \ell M_{\ell+1} M'_\ell}{2h^2 r^2} \right] \sin(u \pm \theta). \quad (37)
\end{aligned}$$

In the original expansion to determine $\psi^{(2)}$, terms such as $G_{\ell+1}$ and $M'_{\ell+1}$ were not multiplied by an ℓ -order field. But in Eq. (37), these terms are multiplied by the square of an ℓ -order field and can then be considered higher-order. In Eq. (37) the $\sin(u \pm \theta)$ terms can be considered fourth-order instead of third-order. The use of this assumption will be used throughout.

However, the above assumption does not imply that all squared ℓ -order terms should be ignored. For example, assuming that the following is contained in a first-order expansion

$$0 = M'_\ell \sin u + \frac{[M'_\ell \sin u]^2}{hr} + \frac{[M'_\ell \sin u]^3}{h^2 r^2} + \dots, \quad (38)$$

one should retain the squared term. According to the above assumption, the $M'_\ell \sin u$ term must be multiplied by the square of an ℓ -order field before it can be ignored. Thus, the cubed term in Eq. (38) can be ignored.

The assumption used for the remainder of the derivation can be generally stated. Terms such as $M_{\ell+1}$, $f(r)$, and a/R can be ignored if multiplied by the square of an ℓ -order field. However, the square of an ℓ -order field must be retained if it does not multiply other terms such as $M_{\ell+1}$, $f(r)$, or a/R .

For the case $M_{\ell-1} = M_0$, $\psi^{(2)}$ remains unchanged. However, Eq. (36) must be changed because

$$B_z^{(1)} \frac{\partial}{\partial z} \psi^{(1)} = - B^{(0)} M_0 \cos(hz) [-hrM_1' \sin(\theta - hz)]$$

does not equal zero. This results in another $\sin \theta$ term which gives

$$\left(\eta - \frac{\gamma}{h^2 r^2} \right) \sin \theta = \frac{M_0 M_1' \sin(\pm \theta)}{2} + \frac{M_1' G_0' \sin(\pm \theta)}{2hr} + \frac{M_0 M_1' \sin(\pm \theta)}{2h^2 r^2} \quad (39)$$

for the $M_{\ell-1} = M_0$ case.

One can now find the flux amplitudes δ_m by expanding $\psi(r, \theta) = \psi(a, \theta)$ in a Taylor series expansion which can be written as

$$\begin{aligned} \psi(r, \theta) = & \psi^{(1)} + (r - a) \frac{\partial}{\partial r} \psi^{(1)} + \frac{(r - a)^2}{2} \frac{\partial^2}{\partial r^2} \psi^{(1)} + \dots \\ & + \psi^{(2)} + (r - a) \frac{\partial}{\partial r} \psi^{(2)} + \frac{(r - a)^2}{2} \frac{\partial^2}{\partial r^2} \psi^{(2)} + \dots \end{aligned} \quad (40)$$

where

$$(r - a) = a\delta_\ell^{(0)} \cos u + a\delta_\ell^{(1)} \cos \theta + a\delta_{\ell+1}^{(1)} \cos(u \pm \theta). \quad (41)$$

Taking the first-order expansion, one obtains

$$\begin{aligned} \psi(r, \theta) = & \psi^{(1)} + a\delta_\ell \cos u \frac{\partial}{\partial r} \psi^{(1)} + \frac{[a\delta_\ell \cos u]^2}{2} \frac{\partial^2}{\partial r^2} + \dots \\ \psi(r, \theta) = & \frac{1}{2} ha^2 - aM_\ell' \cos u + a\delta_\ell \cos u \left[ha - \frac{\ell^2}{ha} M_\ell \cos u \right] \\ & + \frac{[a\delta_\ell \cos u]^2}{2} \left[h + \frac{\ell^2}{ha^2} M_\ell \cos u - \frac{\ell^2}{a} M_\ell' \cos u \right]. \end{aligned} \quad (42)$$

Using $\psi(r, \theta) = \frac{1}{2} ha^2$ and taking the $\cos u$ terms from Eq. (42)

requires that

$$\frac{M'_l}{ha} = \delta_l \left[1 + \left(\frac{l^2}{a} M_l - \frac{l^2}{ha} M'_l \right) \frac{3}{8} \delta_l \right].$$

The last term in the brackets can be ignored, because it is the square of an l -order field. Thus, δ_l is taken as

$$\delta_l = \frac{M'_l}{ha} \quad (43)$$

One now uses the second-order terms in Eq. (40) to find δ and δ_{l+1} . The terms used include

$$\begin{aligned} 0 = & \psi^{(2)} + r^{(1)} \frac{\partial}{\partial r} \psi^{(1)} + r^{(0)} \frac{\partial}{\partial r} \psi^{(2)} + \frac{[r^{(0)} + r^{(1)}]^2}{2} \frac{\partial^2}{\partial r^2} \psi^{(1)} \\ & + \frac{[r^{(0)} + r^{(1)}]^2}{2} \frac{\partial^2}{\partial r^2} \psi^{(2)} + \dots \end{aligned} \quad (44)$$

Ignoring terms that are too small gives

$$\begin{aligned} 0 = & f(r) \cos \theta - aM'_{l+1} \cos(u \pm \theta) - \frac{M'_l f'}{2h} \cos(u \pm \theta) \pm \frac{fM_l l}{2h^2 a} \cos(u \pm \theta) \\ & + [a\delta \cos \theta + a\delta_{l+1} \cos(u \pm \theta)] \left[ha - \left(ha + \frac{l^2}{ha} \right) M_l \cos u \right] \\ & + [a\delta_l \cos u] [f'(r) \cos \theta + G'_{l+1} \cos(u \pm \theta)] \\ & + [a\delta_l \cos u] [a\delta \cos \theta + a\delta_{l+1} \cos(u \pm \theta)] \left[h - \left(hM_l + h^2 aM'_l \right. \right. \\ & \left. \left. - \frac{l^2}{ha^2} M_l + \frac{l^2}{a} M'_l \right) \cos u \right]. \end{aligned}$$

The $\cos \theta$ terms require that

$$\delta = -\frac{f}{ha^2} + \frac{1}{2} \left(1 + \frac{l^2}{h^2 a} \right) \delta_{l+1} M_l - \frac{1}{2} \delta_l \delta_{l+1} - \frac{1}{2ha} \delta_l G'_{l+1}. \quad (45)$$

Ignoring the appropriate $\cos(u \pm \theta)$ terms and solving for δ_{l+1}

gives

$$\delta_{\underline{l+1}} \cos(u \pm \theta) = \left[\frac{M'_{\underline{l+1}}}{ha} - \frac{\delta_l \delta}{2} + \frac{1}{2} \left(1 + \frac{l^2}{h^2 a^2} \right) \delta M_l + \frac{fM_l l}{2h^3 a^4} \right] \cos(u \pm \theta),$$

and using Eq. (45), $f(r)$ can be eliminated.

$$\begin{aligned} \delta_{\underline{l+1}} \cos(u \pm \theta) &= \left[\frac{M'_{\underline{l+1}}}{ha} - \frac{\delta_l \delta}{2} + \frac{1}{2} \left(1 + \frac{l^2}{h^2 a^2} \right) \delta M_l \right] \cos(u \pm \theta) \\ &+ \frac{M_l l}{2h^2 a^2} \left[-\delta + \frac{1}{2} \left(1 + \frac{l^2}{h^2 a^2} \right) \delta_{\underline{l+1}} M_l - \frac{1}{2} \delta_l \delta_{\underline{l+1}} - \frac{1}{2ha} \delta_l G'_{\underline{l+1}} \right] \\ &\cos(u \pm \theta) \end{aligned}$$

Utilizing Eq. (43) allows one to ignore the last three terms. The result is given as

$$\delta_{\underline{l+1}} \cos(u \pm \theta) = \left[\frac{M'_{\underline{l+1}}}{ha} - \frac{\delta_l \delta}{2} + \frac{1}{2} \left(1 + \frac{l^2 \pm l}{h^2 a^2} \right) \delta M_l \right] \cos(u \pm \theta). \quad (46)$$

Both δ_l and $\delta_{\underline{l+1}}$ are valid for all cases including $M_{l-1} = M_0$.

Equation (46) can be written as

$$\begin{aligned} \delta_{\underline{l-1}} \cos(u - \theta) + \delta_{\underline{l+1}} \cos(u + \theta) &= \left[\frac{M'_{\underline{l+1}}}{ha} - \frac{\delta_l \delta}{2} + \frac{1}{2} \left(1 + \frac{l^2 + l}{h^2 a^2} \right) \delta M_l \right] \\ \cos(u + \theta) + \left[\frac{M'_{\underline{l-1}}}{ha} - \frac{\delta_l \delta}{2} + \frac{1}{2} \left(1 + \frac{l^2 - l}{h^2 a^2} \right) \delta M_l \right] &\cos(u - \theta) \end{aligned} \quad (47)$$

Finally, a pressure balance across the plasma interface at $r = a$ is considered. Using a Taylor series expansion allows one to write

$$\begin{aligned}
\bar{B} = & \left[B^{(0)} + B_z^{(1)} + B_z^{(2)} + B_z^{(3)} + r^{(0)} \frac{\partial}{\partial r} B_z^{(1)} + \frac{r^{(0)^2}}{2} \frac{\partial^2}{\partial r^2} B_z^{(1)} + \dots \right. \\
& + r^{(0)} \frac{\partial}{\partial r} B_z^{(2)} + \frac{r^{(0)^2}}{2} \frac{\partial^2}{\partial r^2} B_z^{(2)} + r^{(0)} \frac{\partial}{\partial r} B_z^{(3)} \\
& + \frac{r^{(0)^2}}{2} \frac{\partial^2}{\partial r^2} B_z^{(3)} + r^{(1)} \frac{\partial}{\partial r} B_z^{(1)} + \frac{r^{(1)^2}}{2} \frac{\partial^2}{\partial r^2} B_z^{(1)} \\
& \left. + r^{(1)} \frac{\partial}{\partial r} B_z^{(2)} + r^{(0)} r^{(1)} \frac{\partial^2}{\partial r^2} B_z^{(1)} + r^{(0)} r^{(1)} \frac{\partial^2}{\partial r^2} B_z^{(2)} \right] \\
& + \left[B_r^{(1)} + B_r^{(2)} + B_r^{(3)} + r^{(0)} \frac{\partial}{\partial r} B_r^{(1)} + \frac{r^{(0)^2}}{2} \frac{\partial^2}{\partial r^2} B_r^{(1)} \right. \\
& + r^{(0)} \frac{\partial}{\partial r} B_r^{(2)} + \frac{r^{(0)^2}}{2} \frac{\partial^2}{\partial r^2} B_r^{(2)} + r^{(1)} \frac{\partial}{\partial r} B_r^{(1)} \\
& \left. + r^{(1)} \frac{\partial}{\partial r} B_r^{(2)} + r^{(0)} r^{(1)} \frac{\partial^2}{\partial r^2} B_r^{(1)} \right] \\
& + \left[B_\theta^{(1)} + B_\theta^{(2)} + B_\theta^{(3)} + r^{(0)} \frac{\partial}{\partial r} B_\theta^{(1)} + \frac{r^{(0)^2}}{2} \frac{\partial^2}{\partial r^2} B_\theta^{(1)} \right. \\
& + r^{(0)} \frac{\partial}{\partial r} B_\theta^{(2)} + \frac{r^{(0)^2}}{2} \frac{\partial^2}{\partial r^2} B_\theta^{(2)} + r^{(1)} \frac{\partial}{\partial r} B_\theta^{(1)} \\
& \left. + r^{(1)} \frac{\partial}{\partial r} B_\theta^{(2)} + r^{(0)} r^{(1)} \frac{\partial^2}{\partial r^2} B_r^{(1)} \right]. \tag{48}
\end{aligned}$$

Using the pressure balance,

$$8\pi p + B^2 = \bar{B} \cdot \bar{B} \tag{49}$$

where the left side of Eq. (49) is describing the inside of the plasma at a pressure p . The dot product of \bar{B} is then taken on the outside of the plasma.

It is then possible to write

$$\begin{aligned}
\bar{B} \cdot \bar{B} = & \left[B^{(0)} + B_z^{(1)} + B_z^{(2)} + B_z^{(3)} + r^{(0)} \frac{\partial}{\partial r} B_z^{(1)} + r^{(0)} \frac{\partial}{\partial r} B_z^{(2)} \right. \\
& \left. + r^{(0)} \frac{\partial}{\partial r} B_z^{(3)} + r^{(1)} \frac{\partial}{\partial r} B_z^{(2)} + r^{(0)} r^{(1)} \frac{\partial^2}{\partial r^2} B_z^{(2)} \right]^2 \\
& + \left[B_r^{(1)} + B_r^{(2)} + r^{(0)} \frac{\partial}{\partial r} B_r^{(1)} + r^{(0)} \frac{\partial}{\partial r} B_r^{(2)} \right. \\
& \left. + r^{(1)} \frac{\partial}{\partial r} B_r^{(1)} + r^{(0)} r^{(1)} \frac{\partial^2}{\partial r^2} B_r^{(1)} \right]^2 \\
& + \left[B_\theta^{(1)} + B_\theta^{(2)} + r^{(0)} \frac{\partial}{\partial r} B_\theta^{(1)} + r^{(0)} \frac{\partial}{\partial r} B_\theta^{(2)} \right. \\
& \left. + r^{(1)} \frac{\partial}{\partial r} B_\theta^{(1)} + r^{(0)} r^{(1)} \frac{\partial^2}{\partial r^2} B_\theta^{(1)} \right]^2 \quad (50)
\end{aligned}$$

where terms that are too small have to be deleted. All products involving $r^{(0)2}$ are too small according to the assumptions being used.

In the special case of $M_{\ell-1} = M_0$ and $B_z^{(1)}$ is nonzero, the derivative

$$\frac{\partial}{\partial r} B_z^{(1)} = \frac{\partial}{\partial r} M_0 \cos hz = hM_0' \cos hz$$

is a third-order term. Thus, all terms in Eq. (50) smaller than $r^{(0)} \frac{\partial}{\partial r} B_z^{(1)}$ can be neglected.

By definition

$$\beta = \frac{p}{B_0^2/8\pi} \quad (51)$$

where p is the zero-order plasma pressure.

Equation (50) must be conserved for $B^{(0)} = B_0$ and $B^{(0)} = (1 - \beta)^{1/2} B_0$ as derived from Eq. (49) and Eq. (51).

The following will not be valid for the special case when $M_{\ell-1} = M_0$. The second-order terms must be zero for a stable plasma configuration. The second-order expansion consists of

$$\begin{aligned}
0 = & 2B^{(0)} B_z^{(2)} + 2B^{(0)} r^{(0)} \frac{\partial}{\partial r} B_z^{(2)} + B_r^{(1)2} \\
& + 2B_r^{(1)} r^{(0)} \frac{\partial}{\partial r} B_r^{(1)} + B_\theta^{(1)2} + 2B_\theta^{(1)} r^{(0)} \frac{\partial}{\partial r} B_\theta^{(1)}. \quad (52)
\end{aligned}$$

Substituting in the appropriate values from Eqs. (6-12) gives

$$\begin{aligned}
0 = & -2B^{(0)2} M_\ell \cos u - 2B^{(0)2} a \delta_\ell \cos u h M'_\ell \cos u \\
& + B^{(0)2} [M'_\ell \sin u]^2 + 2B^{(0)2} M'_\ell \sin u [a \delta_\ell \cos u] [h M''_\ell \sin u] \\
& + \frac{B^{(0)2} \ell^2}{h^2 a^2} M_\ell^2 \cos^2 u + \frac{2\ell B^{(0)}}{ha} M_\ell \cos u [a \delta_\ell \cos u] \\
& \left[-\frac{\ell B^{(0)}}{ha^2} M_\ell \cos u + \frac{\ell B^{(0)}}{a} M'_\ell \cos u \right].
\end{aligned}$$

Taking the $\cos u$ terms, all expressions can be considered higher-order except

$$-2B^{(0)2} M_\ell \cos u.$$

Imposing the condition that $B^{(0)} = B_0$ and $B^{(0)} = (1 - \beta)^{1/2} B_0$ gives

$$B^{(0)2} M_\ell^{\text{OUT}} \cos u = (1 - \beta) B^{(0)2} M_\ell^{\text{IN}} \cos u$$

where the superscripts denote the outside and inside of the plasma.

Thus, it is seen that

$$M_\ell^{\text{OUT}} - (1 - \beta) M_\ell^{\text{IN}} = 0 \quad (53)$$

The third-order terms consist of

$$\begin{aligned}
0 = & 2B^{(0)} B_z^{(3)} + 2B^{(0)} r^{(0)} \frac{\partial}{\partial r} B_z^{(3)} + 2B^{(0)} r^{(1)} \frac{\partial}{\partial r} B_z^{(2)} \\
& + 2B^{(0)} r^{(0)} r^{(1)} \frac{\partial^2}{\partial r^2} B_z^{(2)} + 2B_r^{(1)} B_r^{(2)} + 2B_r^{(1)} r^{(1)} \frac{\partial}{\partial r} B_r^{(1)} \\
& + 2B_\theta^{(1)} B_\theta^{(2)} + 2B_\theta^{(1)} r^{(1)} \frac{\partial}{\partial r} B_\theta^{(1)} \quad (54)
\end{aligned}$$

where all terms multiplied by the square of an ℓ -order field have been ignored. Substituting in the values gives

$$\begin{aligned}
0 = & -2B^{(0)2} \left[M_{\ell+1} \cos(u \pm \theta) + \frac{a}{R} \cos \theta \right] - 2B^{(0)2} [a\delta_\ell \cos u] \\
& \left[hM'_{\ell+1} \cos(u \pm \theta) + \frac{1}{R} \cos \theta \right] \\
& - 2B^{(0)2} [a\delta_{\ell+1} \cos(u \pm \theta) + a\delta \cos \theta] [hM'_\ell \cos u] \\
& - 2B^{(0)2} [a\delta_\ell \cos u] [a\delta_{\ell+1} \cos(u \pm \theta) + a\delta \cos \theta] [h^2 M''_\ell \cos u] \\
& + 2B^{(0)2} [M'_\ell \sin u] \left[M'_{\ell+1} \sin(u \pm \theta) + \left(\eta - \frac{\gamma}{h^2 a^2} \right) \sin \theta \right] \\
& + 2B^{(0)2} [M'_\ell \sin u] [a\delta_{\ell+1} \cos(u \pm \theta) + a\delta \cos \theta] [hM''_\ell \sin u] \\
& + 2B^{(0)2} \left[\frac{\ell}{ha} M_\ell \cos u \right] \left[\frac{(\ell+1)}{ha} M_{\ell+1} \cos(u \pm \theta) + \left(\eta + \frac{\gamma}{h^2 a^2} \right) \cos \theta \right] \\
& + 2B^{(0)2} \left[\frac{\ell}{ha} M_\ell \cos u \right] [a\delta_{\ell+1} \cos(u \pm \theta) + a\delta \cos \theta] \\
& \left[\frac{\ell}{a} M'_\ell \cos u - \frac{\ell}{ha^2} M_\ell \cos u \right].
\end{aligned}$$

Taking the $\cos(u \pm \theta)$ terms gives

$$\begin{aligned}
& -2B^{(0)2} M_{\ell+1} \cos(u \pm \theta) - B^{(0)2} \frac{a}{R} \delta_\ell \cos(u \pm \theta) \\
& - B^{(0)2} ha M'_\ell \cos(u \pm \theta),
\end{aligned}$$

and imposing the boundary conditions $B^{(o)} = B_o$ and $B^{(o)} = (1 - \beta)^{1/2} B_o$ gives

$$[M_{\underline{l+1}}^{OUT}] \cos(u \pm \theta) - (1 - \beta) [M_{\underline{l+1}}^{IN}] \cos(u \pm \theta) = - \frac{\beta}{2} \delta_l \frac{a}{R} + \delta h^2 a^2 \cos(u \pm \theta). \quad (55)$$

Finally, one takes the $\cos \theta$ terms and obtains

$$\begin{aligned} 0 = & - 2B^{(o)2} \frac{a}{R} \cos \theta - B^{(o)2} h a \delta_l M'_{\underline{l+1}} \cos \theta \\ & - B^{(o)2} h a \delta_{\underline{l+1}} M'_l \cos \theta + B^{(o)2} h a \delta_l M'_{\underline{l+1}} \cos \theta \\ & + B^{(o)2} \frac{l(l \pm 1)}{h^2 a^2} M_l M_{\underline{l+1}} \cos \theta - B^{(o)2} h^2 a^2 \delta \delta_l M''_l \cos \theta \\ & + B^{(o)2} l^2 M_l \delta_l \delta \cos \theta - B^{(o)2} \frac{l^2}{h^2 a^2} M_l^2 \delta \cos \theta \\ & + B^{(o)2} h^2 a^2 \delta_l \delta M''_l \cos \theta. \end{aligned}$$

Imposing the necessary boundary condition gives

$$\begin{aligned} \frac{2a}{R} = & - \beta h^2 a^2 \delta_{\underline{l+1}} \delta_l - l^2 \delta_l \delta \left[(1 - \beta) M_l^{IN} - M_l^{OUT} \right] \\ & + \frac{l^2}{h^2 a^2} \delta \left[(1 - \beta) M_l^{2IN} - M_l^{2OUT} \right] \\ & - \frac{l(l \pm 1)}{h^2 a^2} \left[(1 - \beta) M_l^{IN} M_{\underline{l+1}}^{IN} - M_l^{OUT} M_{\underline{l+1}}^{OUT} \right]. \quad (56) \end{aligned}$$

Using Eq. (53) and Eq. (54) it is seen that

$$M_l^{OUT} \cos u - (1 - \beta) M_l^{IN} \cos u = 0$$

and

$$\begin{aligned} M_{\underline{l+1}}^{OUT} M_l^{OUT} \cos(u \pm \theta) \cos u = & (1 - \beta) M_{\underline{l+1}}^{2IN} M_l^{2IN} \cos(u \pm \theta) \cos u \\ & - \frac{\beta(1 - \beta)}{2} \delta_l M_l^{IN} \left[\frac{a}{R} + \delta h^2 a^2 \right] \cos u \cos(u \pm \theta) \end{aligned}$$

which gives

$$M_{\underline{l+1}}^{\text{OUT}} M_l^{\text{OUT}} = (1 - \beta)^2 M_{\underline{l+1}}^{\text{IN}} M_l^{\text{IN}} - \beta(1 - \beta) \delta_l M_l^{\text{IN}} \left[\frac{a}{R} + \delta h^2 a^2 \right].$$

Substituting these into Eq. (56) gives

$$\begin{aligned} \frac{2\beta a}{R} = & - \beta h^2 a^2 \delta_{\underline{l+1}} \delta_l + \frac{l^2}{h^2 a^2} \delta \beta (1 - \beta) M_l^{\text{IN}^2} \\ & - \frac{\beta(1 - \beta) l(l \pm 1)}{h^2 a^2} M_l^{\text{IN}} M_{\underline{l+1}}^{\text{IN}} \\ & - \beta(1 - \beta) \delta_l M_l^{\text{IN}} \left[\frac{a}{R} + \delta h^2 a^2 \right] \left[\frac{l^2}{h^2 a^2} \right]. \end{aligned} \quad (57)$$

Ignoring the a/R term on the right side of Eq. (57) because it is multiplied by the square of an l -order field, and substituting in for $\delta_{\underline{l+1}}$ from Eq. (46) gives

$$\begin{aligned} \frac{2a}{R} = & - ha \delta_l M_{\underline{l+1}}^{\text{IN}} - (1 - \beta) M_l^{\text{IN}} \left[M_{\underline{l+1}}^{\text{IN}} \frac{l(l \pm 1)}{h^2 a^2} \right] + (ha)^2 \delta_l^2 \delta \\ & + (1 - \beta) \frac{l^2}{h^2 a^2} \delta M_l^{\text{IN}^2} - \delta \delta_l M_l^{\text{IN}} (2 - \beta) l^2 \\ & - \delta \delta_l M_l^{\text{IN}} h^2 a^2. \end{aligned} \quad (58)$$

The special case $M_{l-1} = M_0$ will now be treated. In this case $B_z^{(1)}$ is not zero, and one obtains in the first-order

$$0 = 2B^{(0)} B_z^{(1)} = - 2B^{(0)2} M_0 \cos hz,$$

or

$$M_0^{\text{OUT}} - (1 - \beta) M_0^{\text{IN}} = 0. \quad (59)$$

However, the third-order terms

$$- B^{(0)2} \frac{a}{R} \delta_1 \cos hz - B^{(0)2} ha \delta_1' \cos hz$$

should also be included with Eq. (59). This gives

$$M_o^{OUT} \cos hz - (1 - \beta)M_o^{IN} \cos hz = -\frac{\beta}{2} \delta_1 \left[\frac{a}{R} + \delta h^2 a^2 \right] \cos hz.$$

This is the same result that is obtained for the general case given by Eq. (55). Thus, Eq. (55) is valid for all cases including $M_{\ell-1} = M_o$.

The term $B_z^{(1)2}$ must be added to the second-order expansion, but this doesn't add any $\cos u$ terms. Thus, Eq. (53) is valid for all cases.

In the third-order, one must add the terms

$$2B^{(0)}_r{}^{(0)} \frac{\partial}{\partial r} B_z^{(1)} + 2B_z^{(1)} B_z^{(2)}$$

for the case $M_{\ell-1} = M_o$.

One obtains the $\cos \theta$ terms given below as

$$\begin{aligned} & - 2B^{(0)2} \frac{a}{R} \cos \theta - B^{(0)2} h a \delta_1 M'_2 \cos \theta \\ & - B^{(0)2} h^2 a^2 \delta_1 (\delta_o + \delta_2) + B^{(0)2} h a \delta_1 (M'_o + M'_2) \cos \theta \\ & - B^{(0)2} \frac{2}{h^2 a^2} M_1 M_2 \cos \theta - B^{(0)2} h a \delta_1 M'_o \cos \theta \\ & + B^{(0)2} M_o M_1 \cos \theta - B^{(0)2} h^2 a^2 \delta \delta_1 M''_1 \cos \theta \\ & + B^{(0)2} M_1 \delta_1 \delta \cos \theta - B^{(0)2} \frac{M_1^2}{h^2 a^2} \delta \cos \theta + B^{(0)2} h^2 a^2 \delta_1 \delta M''_1 \cos \theta. \end{aligned}$$

Using Eq. (53) and Eq. (55) and applying the necessary boundary conditions gives

$$\begin{aligned} \frac{2a}{R} = & -h^2 a^2 \delta_1 (\delta_o + \delta_2) + \frac{\delta}{h^2 a^2} (1 - \beta) M_1^{IN^2} - (1 - \beta) M_o^{IN} M_1^{IN} \\ & - (1 - \beta) \frac{2}{h^2 a^2} M_1^{IN} M_2^{IN} - (1 - \beta) \delta_1 M_1 \delta \left[1 + \frac{h^2 a^2}{2} \right]. \end{aligned} \quad (60)$$

In Eq. (60), the term

$$(1 - \beta) \delta_1 M_1 \delta \frac{h^2 a^2}{2}$$

is actually a fifth-order quantity. It will be seen that fifth-order terms are important for the $\ell - 1 = 0$ case. Thus, one should add all fourth-order and fifth-order terms to Eq. (60). There are no fourth-order $\cos \theta$ terms. However, a number of fifth-order expressions exist that are rather complicated and make the expansion calculations very difficult to do. Thus, only one of the simpler fifth-order expressions will be retained. This is given by

$$2B_z^{(2)} B_z^{(3)} = M_1 M_2 \cos \theta.$$

Including this expression in Eq. (60) gives

$$\begin{aligned} \frac{2a}{R} = & -ha \delta_1 (M_o^{IN} + M_2^{IN}) - (1 - \beta) M_1^{IN} \left[\left(1 + \frac{2}{h^2 a^2} \right) M_2^{IN} + M_o^{IN} \right] \\ & - (2 - \beta) \delta_1 M_1 \delta [1 + h^2 a^2] + h^2 a^2 \delta_1^2 \delta + \frac{\delta}{h^2 a^2} (1 - \beta) M_1^{IN^2} \end{aligned} \quad (61)$$

where Eq. (47) has been used. Equation (61) is merely a generalized form of Eq. (58) that has been made to include $M_{\ell-1} = M_o$. This makes it possible to write

$$\begin{aligned} \frac{2a}{R} = & -ha\delta_{l+1}^{M',IN} - (1-\beta)M_l^{IN}M_{l+1}^{IN} \left[1 + \frac{l(l+1)}{h^2a^2} \right] + (ha)^2\delta_l^2\delta \\ & + (1-\beta)\frac{l^2}{h^2a^2}\delta M_l^{IN^2} - \delta\delta_l M_l^{IN}(2-\beta)[l^2+h^2a^2]. \end{aligned} \quad (62)$$

for all cases, including $M_{l-1} = M_0$.

It is now necessary to calculate the coefficients C_l , D_l , C_{l+1} , and D_{l+1} .

Setting $\delta_l^{IN} = \delta_l^{OUT}$ from Eq. (43) gives

$$C_l^{OUT}I_l' + D_l^{OUT}K_l' = C_l^{IN}I_l' \quad (63)$$

where D_l^{IN} must be zero, because K_l' goes to infinity as r goes to zero.

Using the pressure balance at $r = a$ provided Eq. (53), which can be written as

$$C_l^{OUT}I_l + D_l^{OUT}K_l = (1-\beta)C_l^{IN}I_l. \quad (64)$$

Using Eq. (63) and Eq. (64) allows one to eliminate C_l^{IN} . Solving for D_l^{OUT} gives

$$D_l^{OUT} = \frac{C_l^{OUT} \left[-\beta \frac{I_l}{K_l} \right]}{1 - \frac{(1-\beta)I_l K_l'}{K_l I_l'}}.$$

The expression for D_l^{OUT} can then be substituted into δ_l where

$$\delta_l = \frac{1}{ha} [C_l^{OUT}I_l' + D_l^{OUT}K_l'].$$

This results in the expression

$$\delta_l = C_l^{OUT} \left\{ (ha)^2 K_l \left[1 - (1-\beta) \frac{I_l K_l'}{K_l I_l'} \right] \right\}^{-1} \quad (65)$$

where the identity

$$I'_{lK_l} - I_{lK'_l} = \frac{1}{ha} \quad (66)$$

has been used.

It is also seen that

$$\delta_l = \frac{1}{ha} C_{lI'_l}^{IN}, \quad (67)$$

and

$$M_l^{IN} = C_{lI_l}^{IN}.$$

Thus, C_l^{IN} can be eliminated to obtain

$$M_l^{IN} = ha \frac{I_l}{I'_l} \delta_l. \quad (68)$$

In a similar way, one can derive the $l \pm 1$ quantities by first setting $\delta_{l+1}^{OUT} = \delta_{l+1}^{IN}$. From Eq. (46) it is found that

$$[C_{l+1I'_{l+1}}^{OUT} + D_{l+1K'_{l+1}}^{OUT}] = [C_{l+1I_{l+1}}^{IN}] + \frac{1}{2} \beta h^2 a^2 \left[1 + \frac{l^2 \pm l}{h^2 a^2} \right] \delta_l \frac{I_l}{I'_l} \quad (69)$$

where Eq. (53) and Eq. (67) are used.

The last equation comes from the pressure balance. Using Eq. (55) it is seen that

$$[C_{l+1I_{l+1}}^{OUT} + D_{l+1K_{l+1}}^{OUT}] = (1 - \beta) C_{l+1I_{l+1}}^{IN} - \frac{\beta}{2} \delta_l \left[\frac{a}{R} + \beta h^2 a^2 \right]. \quad (70)$$

Going through the same procedure that was used to derive Eq. (65) gives

$$M_{l+1} = W_{l+1} + Z_{l+1} \quad (71)$$

where

$$Z_{\underline{l+1}} = \frac{C_{\underline{l+1}}^{\text{OUT}}}{\text{haK}'_{\underline{l+1}} \left[\frac{I'_{\underline{l+1}} K_{\underline{l+1}}}{I_{\underline{l+1}} K'_{\underline{l+1}}} - (1 - \beta) \right]}, \quad (72)$$

and

$$W_{\underline{l+1}} = \frac{\frac{\beta}{2} \delta_{\underline{l}} \left[\frac{a}{R} + \delta n^2 a^2 \right] + \frac{\beta}{2} h^2 a^2 \delta \delta_{\underline{l}} \frac{K_{\underline{l+1}} I_{\underline{l}}}{K'_{\underline{l+1}} I'_{\underline{l}}} \left[1 + \frac{l(l \pm 1)}{h^2 a^2} \right]}{(1 - \beta) - \frac{I'_{\underline{l+1}} K_{\underline{l+1}}}{I_{\underline{l+1}} K'_{\underline{l+1}}}}. \quad (73)$$

It is also seen that

$$M_{\underline{l+1}}^{\prime \text{IN}} = C_{\underline{l+1}}^{\text{IN}} I'_{\underline{l+1}},$$

and

$$M_{\underline{l+1}}^{\text{IN}} = C_{\underline{l+1}}^{\text{IN}} I_{\underline{l+1}},$$

which gives

$$M_{\underline{l+1}} = \frac{I_{\underline{l+1}}}{I'_{\underline{l+1}}} M_{\underline{l+1}}^{\prime \text{IN}}. \quad (74)$$

It is now possible to use the derived equations to express the shift necessary to give toroidal equilibrium. Substituting Eq. (68), Eq. (71), and Eq. (74) into Eq. (62) gives

$$\begin{aligned} \frac{2a}{R} = & -\text{ha} \delta_{\underline{l}} \frac{I'_{\underline{l+1}}}{I_{\underline{l+1}}} [W_{\underline{l+1}} + Z_{\underline{l+1}}] - (1 - \beta) \text{ha} \frac{I_{\underline{l}}}{I'_{\underline{l}}} \delta_{\underline{l}} \\ & \left[(W_{\underline{l+1}} + Z_{\underline{l+1}}) \left(1 + \frac{l(l \pm 1)}{h^2 a^2} \right) \right] \\ & + h^2 a^2 \delta_{\underline{l}}^2 \delta + (1 - \beta) l^2 \delta \frac{I_{\underline{l}}^2}{I_{\underline{l}}'^2} \delta_{\underline{l}}^2 - \delta \delta_{\underline{l}} \text{ha} \frac{I_{\underline{l}}}{I'_{\underline{l}}} \delta_{\underline{l}} (2 - \beta) [l^2 + h^2 a^2]. \end{aligned} \quad (75)$$

Substituting in for $W_{\underline{l+1}}$, one can see that the term involving $\frac{\beta}{2} \delta_l \frac{a}{R}$ can be ignored, because it would be multiplied by the square of an l -order field in the above expression.

The condition for equilibrium is that $\delta = 0$. Taking Eq. (75) with $\delta = 0$ gives

$$\frac{-2}{hR\delta_l} = \left[\frac{I'_{\underline{l+1}}}{I_{\underline{l+1}}} + (1 - \beta) \left(1 + \frac{l(l \pm 1)}{h^2 a^2} \right) \frac{I_l}{I'_l} \right] z_{\underline{l+1}}. \quad (76)$$

In order to plot the various results, it is assumed that a vacuum field exists which implies that

$$D_m = 0, \quad (m = l, l \pm 1).$$

The maximum magnitude of the radial field is just

$$\frac{B_r^{(m)}}{B_o} = C_m I'_m, \quad (m = l, l \pm 1). \quad (77)$$

From Eq. (65) it is easily seen that

$$\frac{1}{\delta_l} \frac{B_r^{(l)}}{B_o} = (ha)^2 I'_{lK_l} \left[1 - (1 - \beta) \frac{I_{lK'_l}}{I'_{lK_l}} \right]. \quad (78)$$

Taking Eq. (46), Eq. (71), and Eq. (74) for $\delta = 0$ gives

$$\delta_{\underline{l+1}} = \frac{M'_{\underline{l+1}}}{ha}$$

and

$$M'_{\underline{l+1}} = \frac{I'_{\underline{l+1}}}{I_{\underline{l+1}}} \frac{C_{\underline{l+1}}^{OUT}}{haK'_{\underline{l+1}}} \left[\frac{I'_{\underline{l+1}K_{\underline{l+1}}}}{I_{\underline{l+1}K_{\underline{l+1}}}} - (1 - \beta) \right].$$

This allows one to write

$$\frac{1}{\delta_{\underline{l+1}}} \frac{B_r^{(\underline{l+1})}}{B_o} = (ha)^2 I_{\underline{l+1}}' K_{\underline{l+1}} \left[1 - (1 - \beta) \frac{I_{\underline{l+1}}' K_{\underline{l+1}}'}{I_{\underline{l+1}}' K_{\underline{l+1}}} \right]. \quad (79)$$

It is then seen that Eq. (78) and Eq. (79) are of the same form, and both can be written as

$$\frac{1}{\delta_m} \frac{B_r^{(m)}}{B_o} = (ha)^2 I_m' K_m \left[1 - (1 - \beta) \frac{I_m' K_m'}{I_m' K_m} \right] \quad (80)$$

where $m = l, l \pm 1 = 0, 1, 2, 3, \dots$

Equation (80) is plotted in Figs. 1-4 on the next few pages for various $ha, m,$ and β values.

Using Eq. (76) for $\delta = 0$ and recognizing that

$$\delta_{\underline{l+1}} = \frac{M_{\underline{l+1}}'}{ha}$$

and

$$M_{\underline{l+1}}' = Z_{\underline{l+1}} \frac{I_{\underline{l+1}}'}{I_{\underline{l+1}}}$$

for $\delta = 0$, allows one to immediately write

$$\frac{R}{a} \delta_l \delta_{\underline{l+1}} = - \frac{2}{h^2 a^2} \frac{1}{\left[1 + (1 - \beta) \left[1 + \frac{l(l \pm 1)}{h^2 a^2} \right] \frac{I_l' I_{\underline{l+1}}}{I_l' I_{\underline{l+1}}} \right]}. \quad (81)$$

Equation (81) is plotted in Figs. 5-8. Substituting Eq. (80) into Eq. (81) gives

$$\frac{R}{a} \frac{B_r^{l, \underline{l+1}}}{B_o^2} = 2(ha)^2 I_l' K_l I_{\underline{l+1}}' K_{\underline{l+1}} \frac{\left[1 - (1 - \beta) \frac{I_{\underline{l+1}}' K_{\underline{l+1}}'}{I_{\underline{l+1}}' K_{\underline{l+1}}} \right] \left[1 - (1 - \beta) \frac{I_l' K_l'}{I_l' K_l} \right]}{\left\{ 1 + (1 - \beta) \left[1 + \frac{l(l \pm 1)}{h^2 a^2} \right] \frac{I_l' I_{\underline{l+1}}}{I_l' I_{\underline{l+1}}} \right\}}. \quad (82)$$

Equation (82) is plotted in Figs. 9-12.

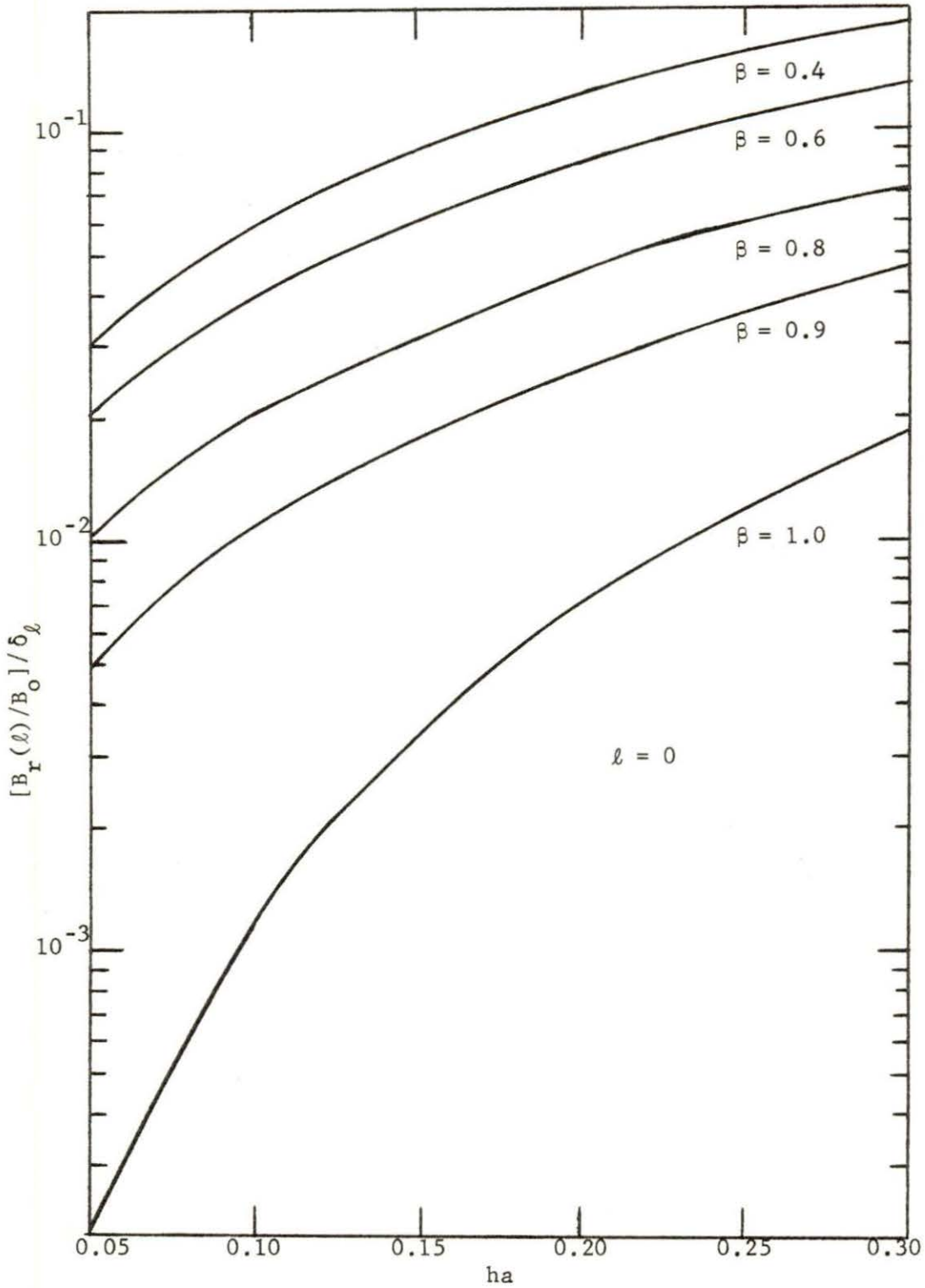


Fig. 1. Ratio of maximum radial field to the plasma perturbation it produces versus ha for $l = 0$.

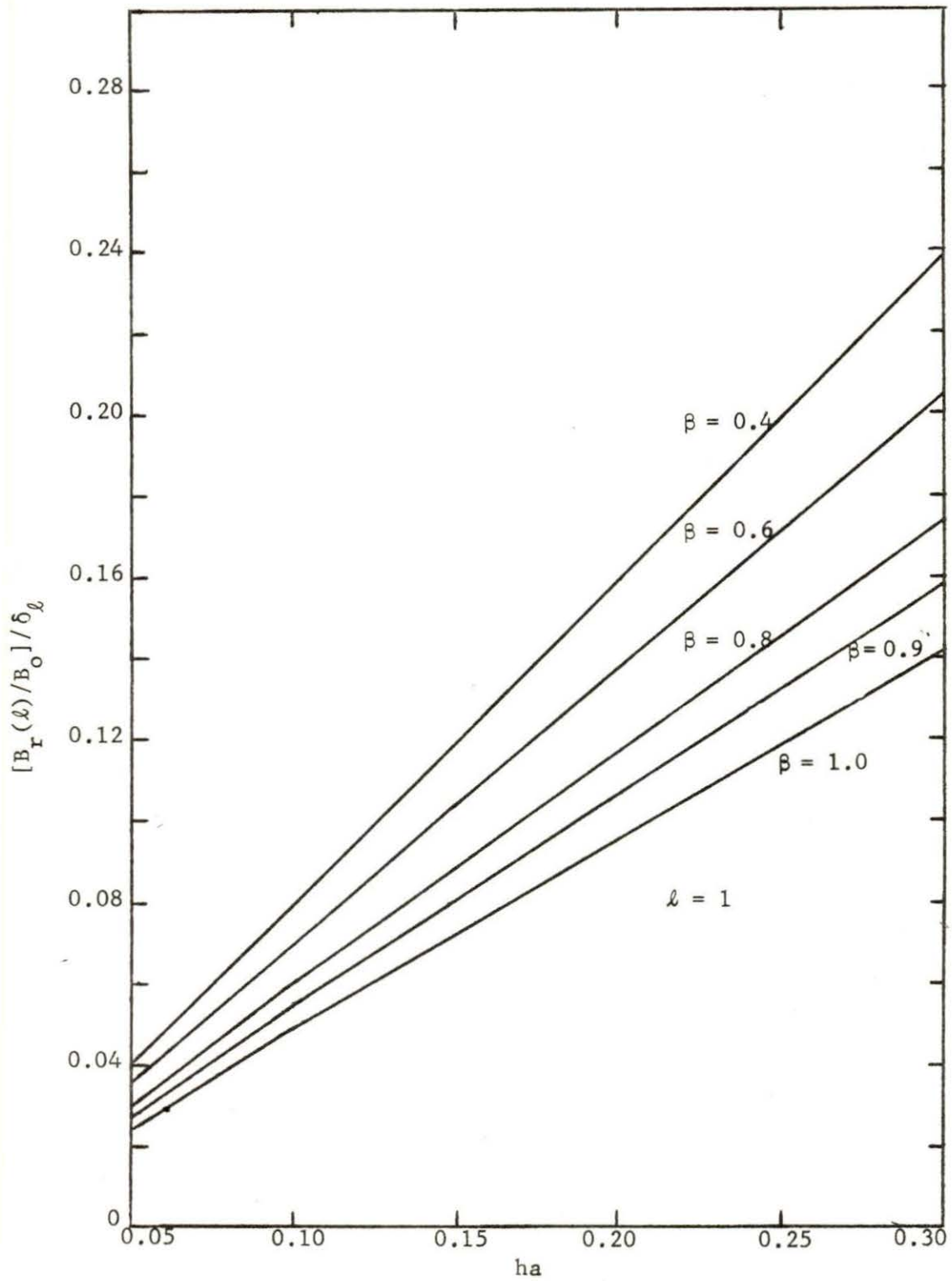


Fig. 2. Ratio of maximum radial field to the plasma perturbation it produces versus ha for $l = 1$.

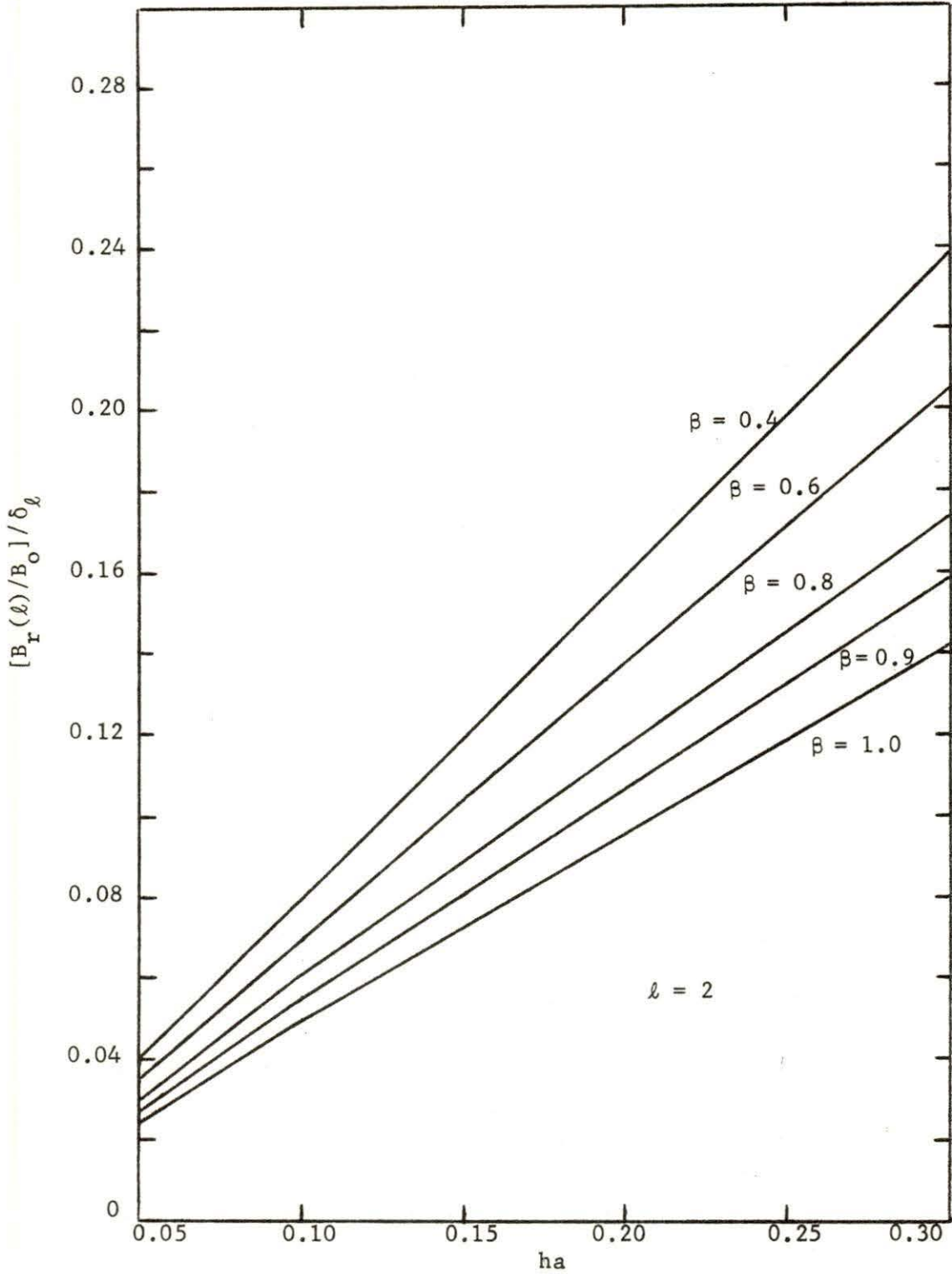


Fig. 3. Ratio of maximum radial field to the plasma perturbation it produces versus ha for $l = 2$.

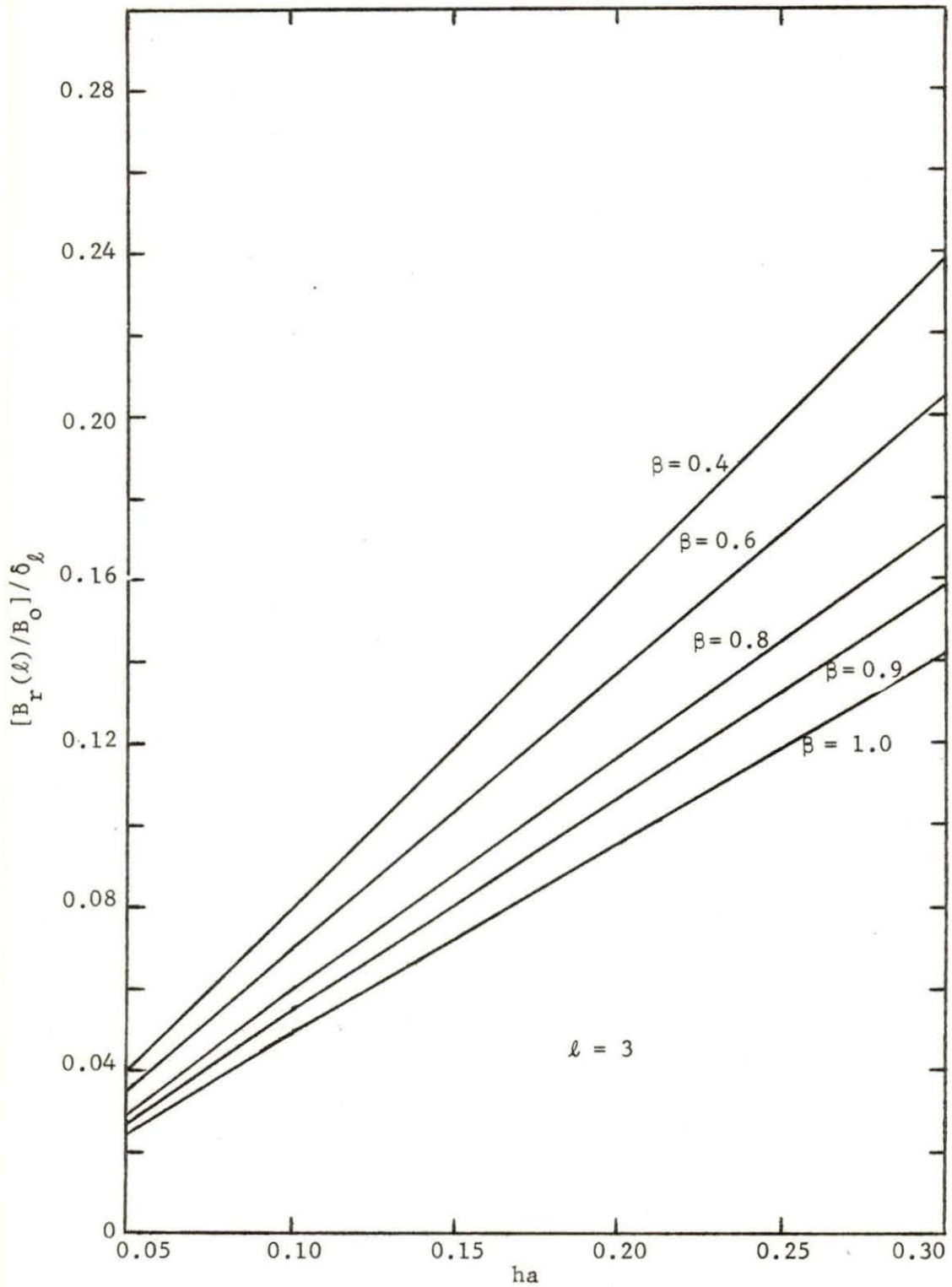


Fig. 4. Ratio of maximum radial field to the plasma perturbation it produces versus ha for $l = 3$.

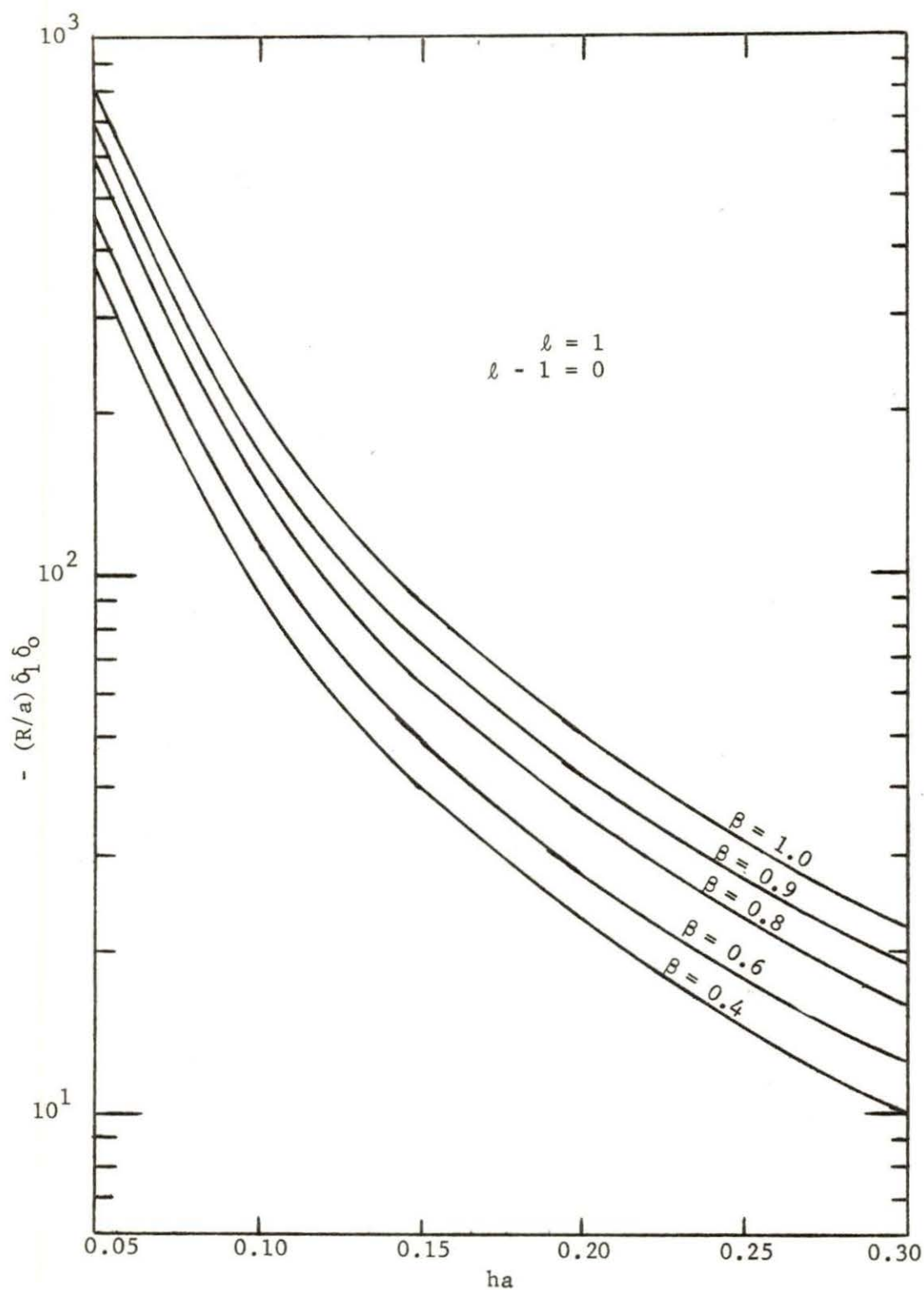


Fig. 5. The quantity $-(R/a) \delta_0 \delta_1$ versus ha necessary for toroidal equilibrium.

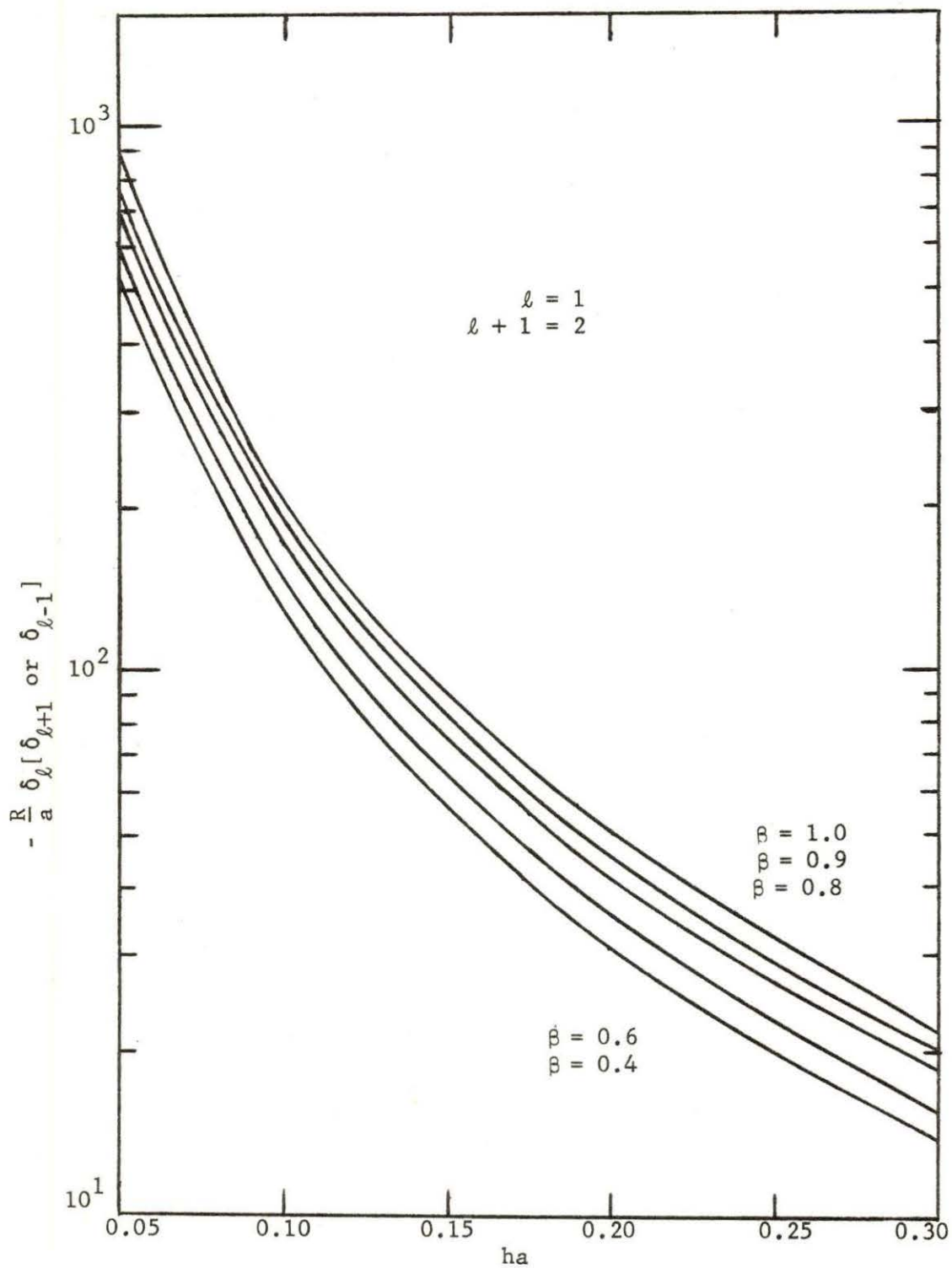


Fig. 6. The quantity $-(R/a)\delta_\ell[\delta_{\ell+1} \text{ or } \delta_{\ell-1}]$ versus ha necessary for toroidal equilibrium.

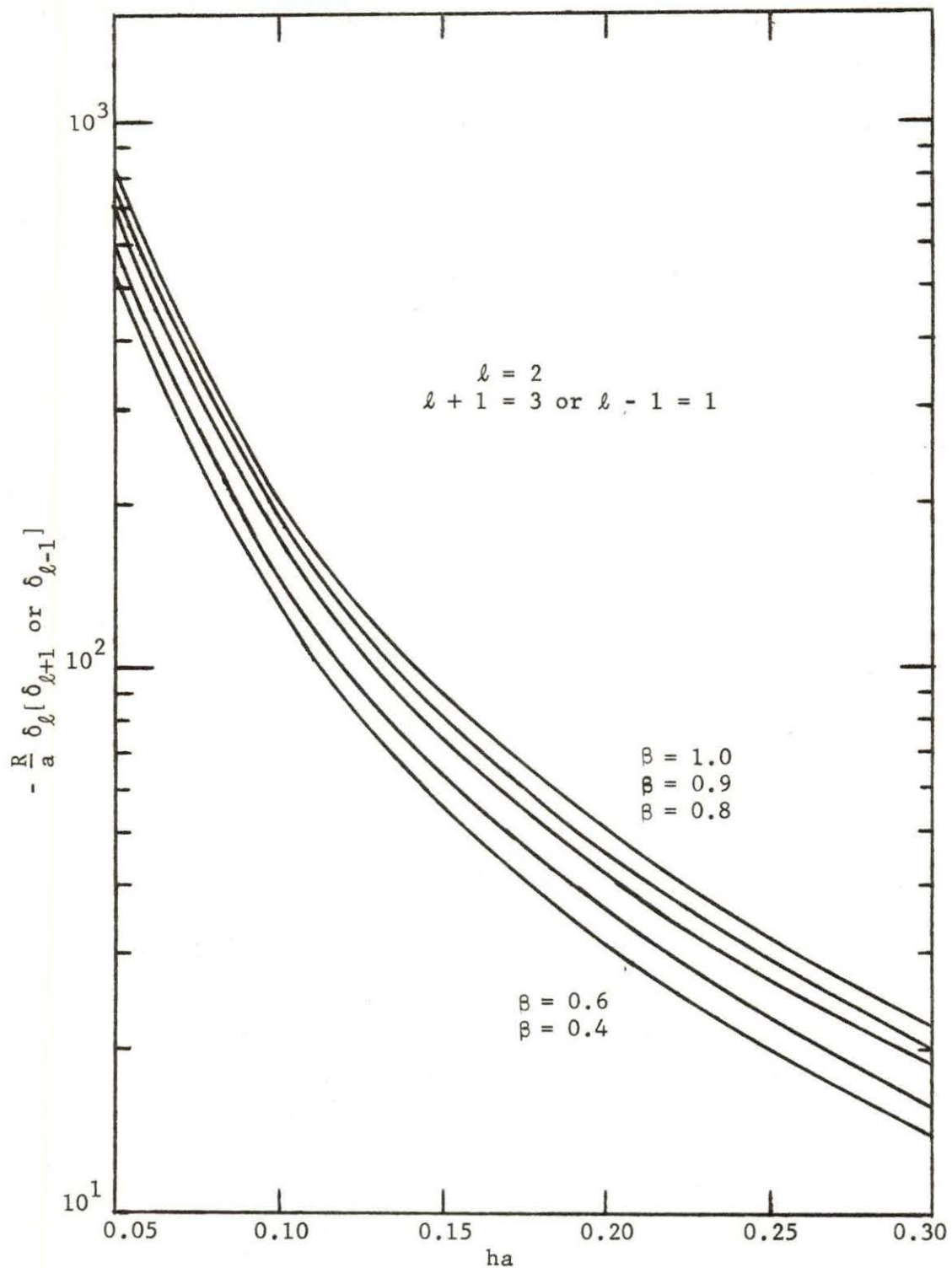


Fig. 7. The quantity $-(R/a)\delta_\ell[\delta_{\ell+1}$ or $\delta_{\ell-1}]$ versus ha necessary for toroidal equilibrium.

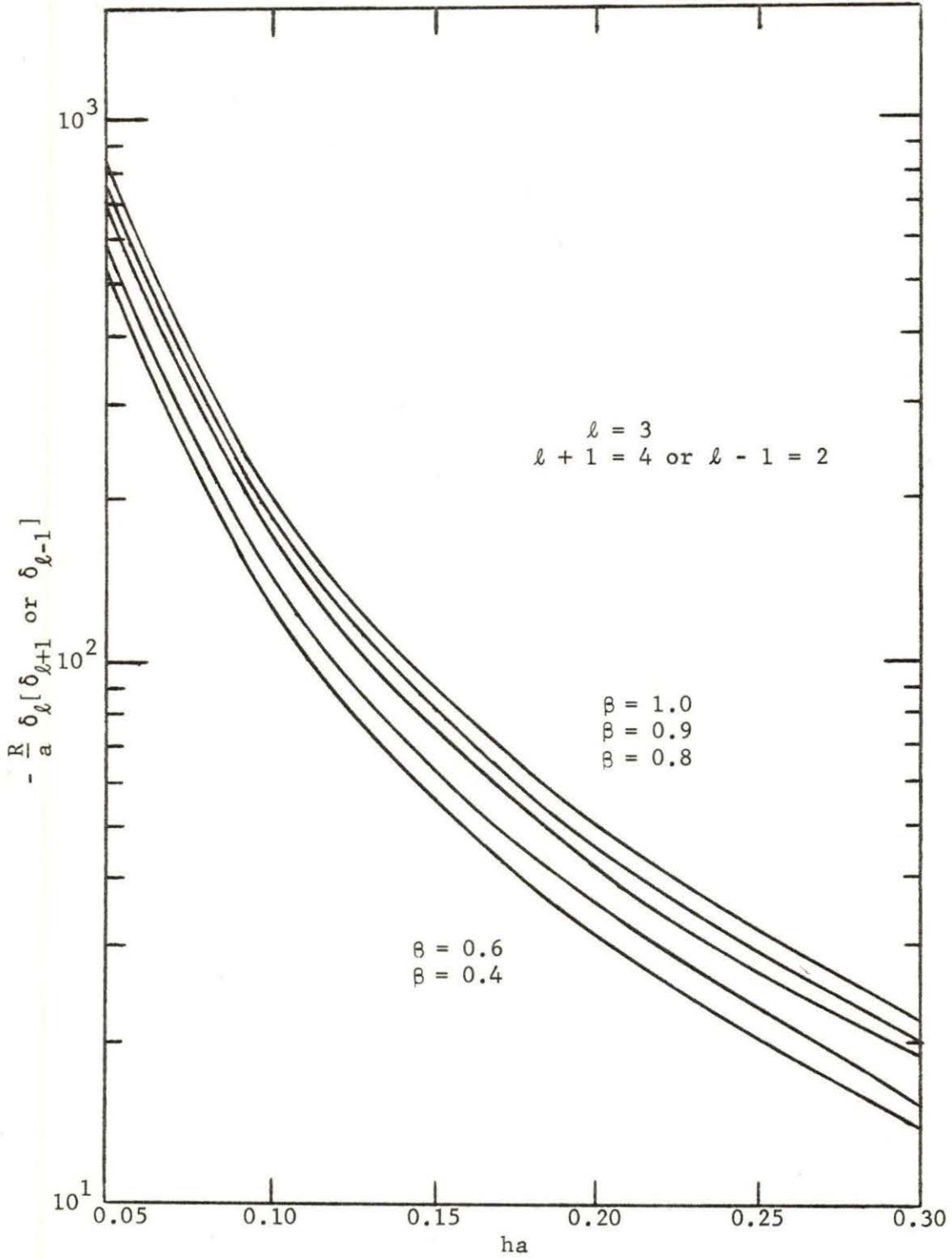


Fig. 8. The quantity $-(R/a) \delta_\ell [\delta_{\ell+1} \text{ or } \delta_{\ell-1}]$ versus ha necessary for toroidal equilibrium.

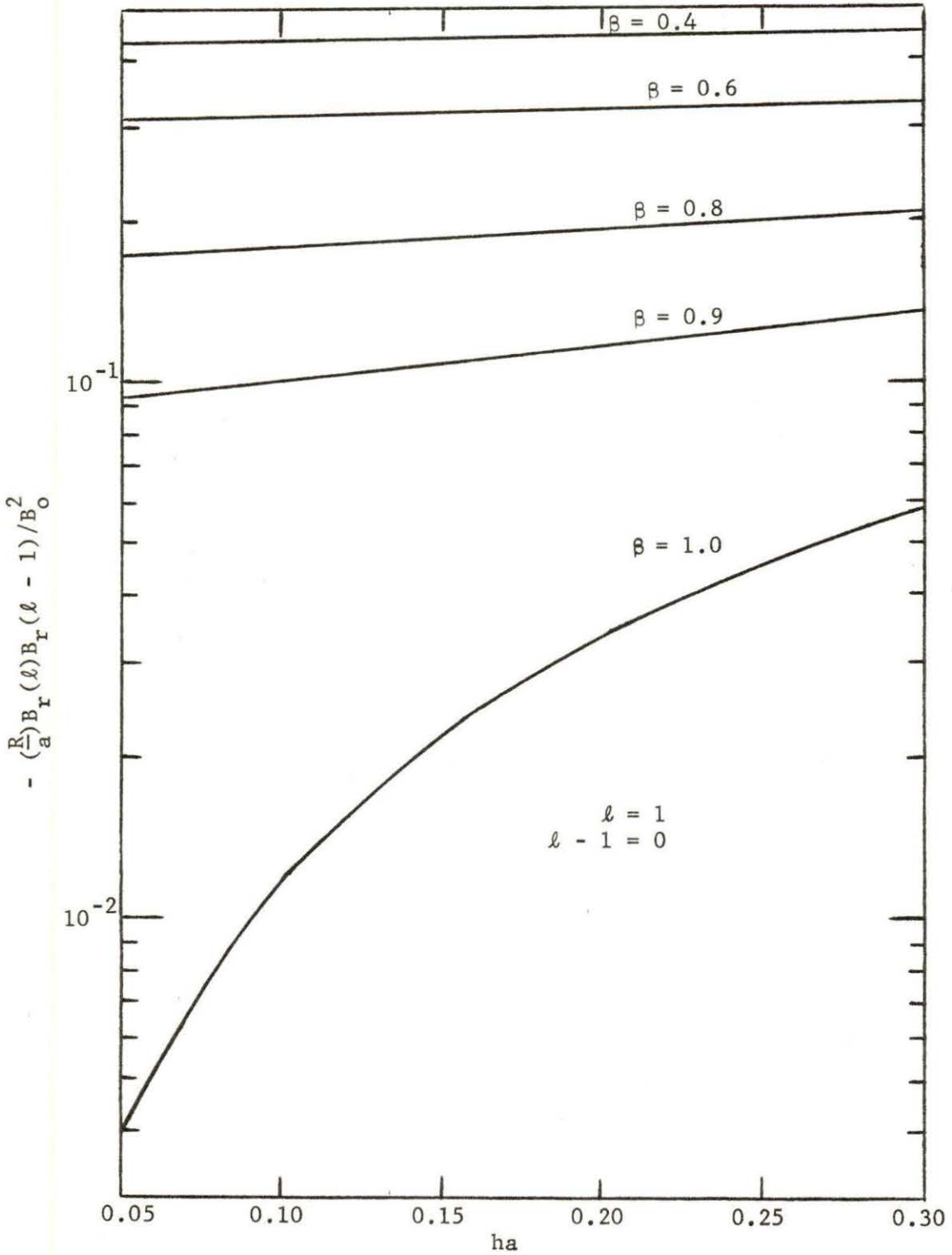


Fig. 9. The quantity $-\left(\frac{R}{a}\right)B_r(l)B_r(l-1)/B_0^2$ versus ha necessary for toroidal equilibrium.

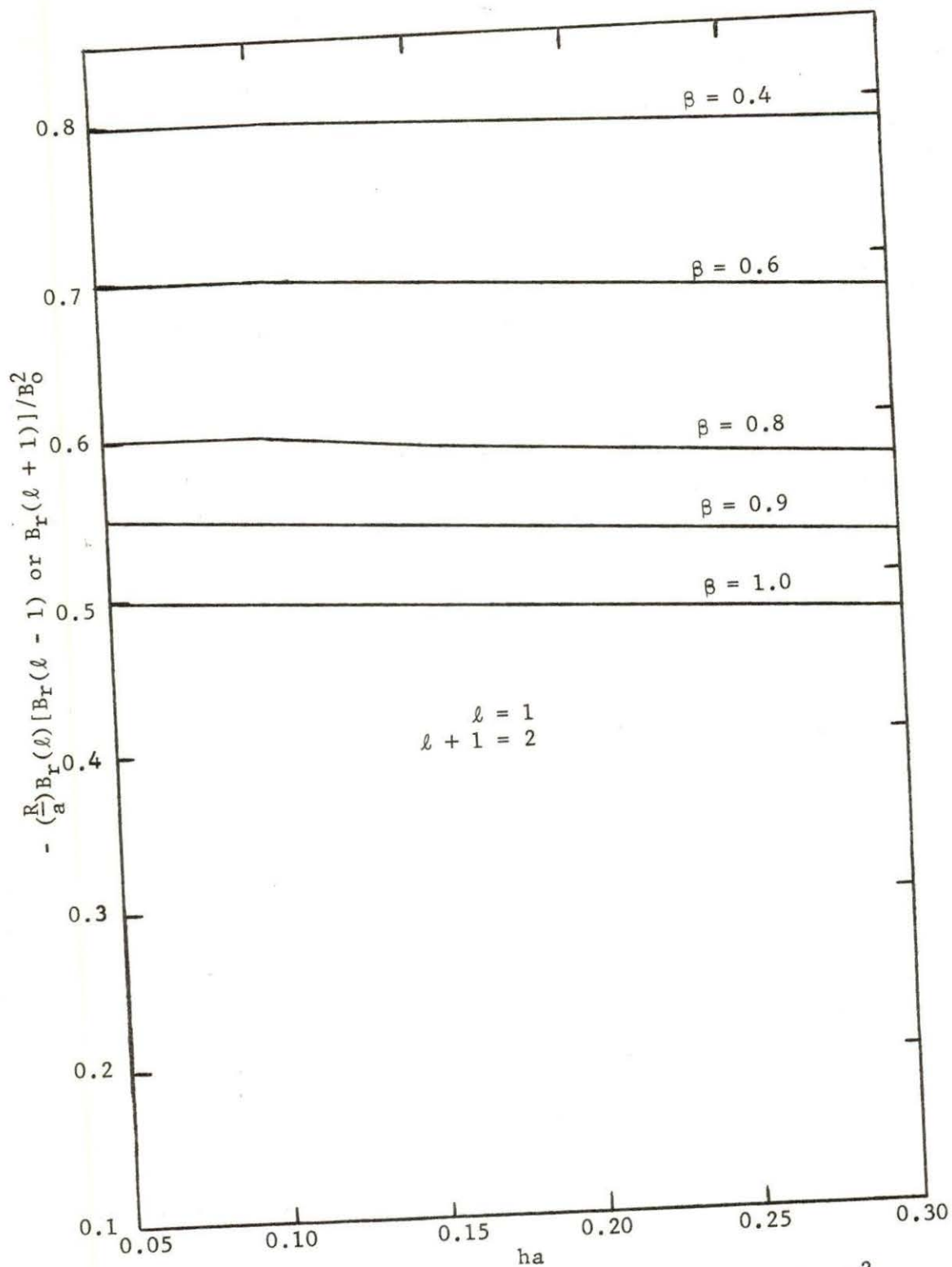


Fig. 10. The quantity $-\frac{R}{a}B_r(l)[B_r(l-1) \text{ or } B_r(l+1)]/B_0^2$ versus ha necessary for toroidal equilibrium.

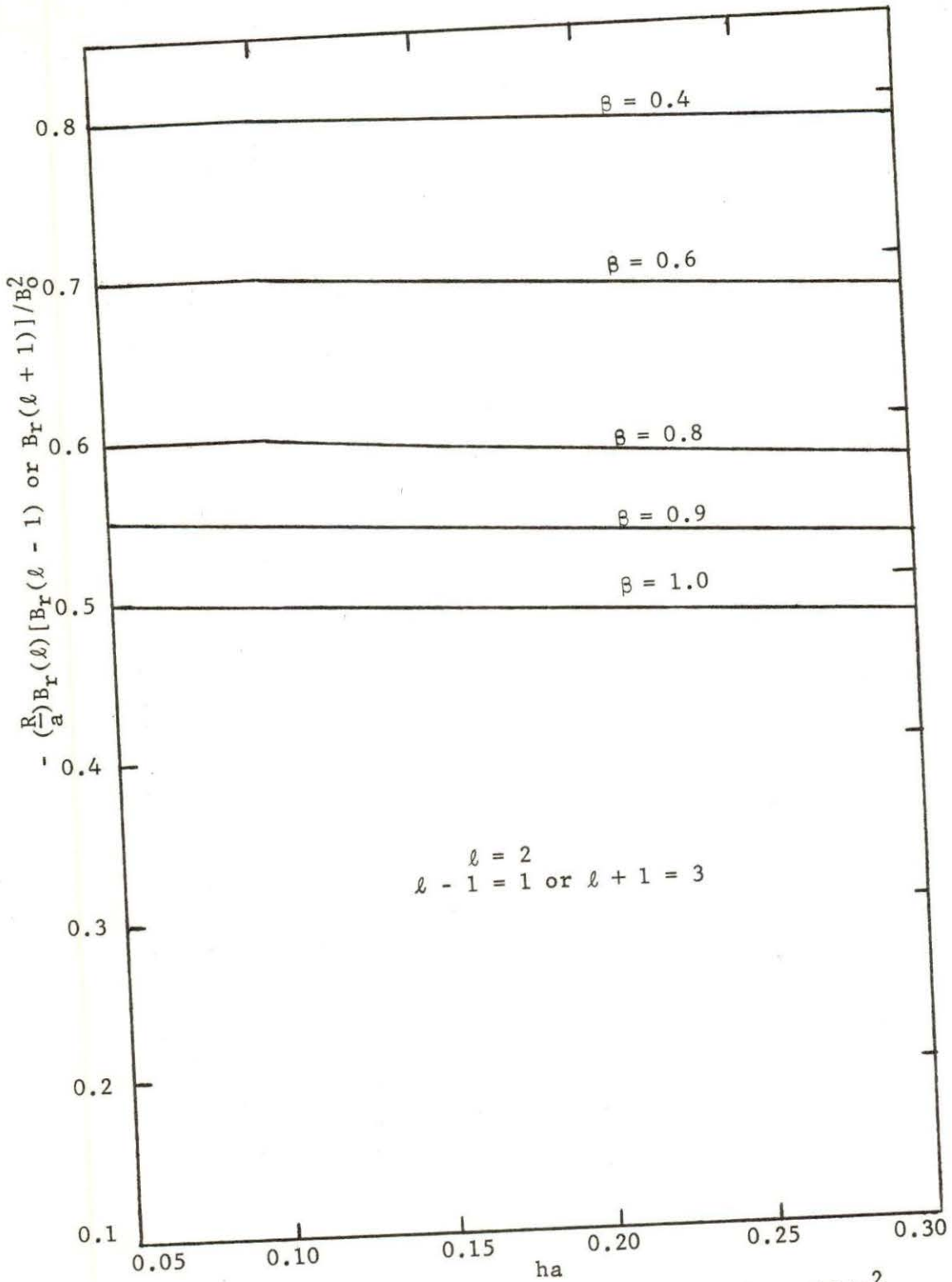


Fig. 11. The quantity $-\frac{R}{a} B_r(l) [B_r(l-1) \text{ or } B_r(l+1)] / B_0^2$ versus ha necessary for toroidal equilibrium.

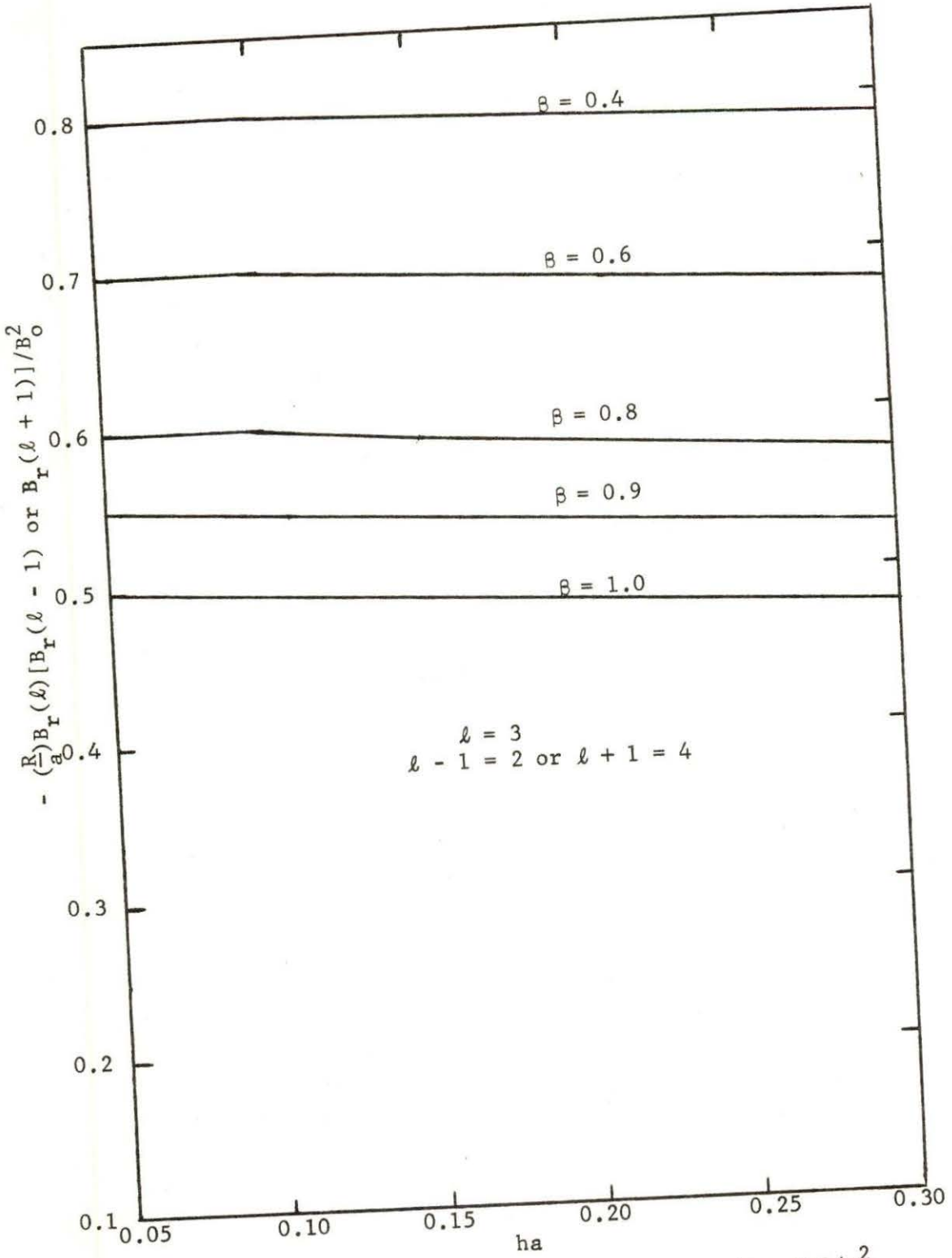


Fig. 12. The quantity $-\frac{R}{a}B_r(l)[B_r(l-1) \text{ or } B_r(l+1)]/B_0^2$ versus ha necessary for toroidal equilibrium.

D. Growth Rates of Instabilities

Multiplying Eq. (49) by $a \cos \theta$ and integrating over θ produces the force per unit length along the plasma column. This procedure takes plasma pressure in force per area and integrates over the plasma area in order to obtain the plasma force. Only the $\cos \theta$ terms don't integrate to zero. The above integration is equivalent to multiplying Eq. (75) by $\beta B_0^2 a/8$.

The balance of forces along the plasma column can then be represented by

$$F_R = F_l + F_{l+1} \quad (83)$$

The forces can then be written as

$$F_R = \frac{\beta B_0^2 a^2}{4R}, \quad (84)$$

$$F_l = -\frac{\beta}{8} B_0^2 h^2 a^2 \delta_l^2 a \delta R_l, \quad (85)$$

where

$$R_l = 1 + \frac{(1-\beta)}{h^2 a^2} l^2 \frac{I_l^2}{I_l'^2} - \frac{1}{ha} \frac{I_l}{I_l'} (2-\beta) [l^2 + h^2 a^2]$$

$$- ha \frac{\beta}{2} \left[\frac{I_{l+1}'}{I_{l+1}} + (1-\beta) \frac{I_l}{I_l'} \left(1 + \frac{l^2 \pm l}{h^2 a^2} \right) \right] \frac{\left[1 + \frac{K_{l+1}}{K_{l+1}} \frac{I_l}{I_l'} \left(1 + \frac{l^2 \pm l}{h^2 a^2} \right) \right]}{\left(1 - \beta \right) - \frac{I_{l+1} K_{l+1}}{I_{l+1} K_{l+1}}}, \quad (86)$$

and

$$F_{l+1} = \frac{\beta}{8} B_0^2 h a^2 \delta_l \left[\frac{I_{l+1}'}{I_{l+1}} + (1-\beta) \left(1 + \frac{l^2 \pm l}{h^2 a^2} \right) \frac{I_l}{I_l'} \right] z_{l+1}. \quad (87)$$

The growth rate of an unstable $m = 1$ displacement given by $\xi = a\delta$ can now be found. By setting

$$\pi a^2 \rho \ddot{\xi} = F_{\ell} \quad (88)$$

where

$$\xi = \xi_0 e^{V_g t},$$

ρ = plasma density,

V_g = growth rate of unstable column,

one finds that

$$V_g^2 = -\frac{\beta}{2} \frac{B_0^2}{4\pi p} h^2 \delta_{\ell}^2 R_{\ell}.$$

This can be written as

$$\frac{V_g}{h V_A \delta_{\ell}} = \left(-\frac{\beta}{2} R_{\ell}\right)^{1/2} \quad (89)$$

where

$$V_A = \frac{B_0}{(4\pi p)^{1/2}} = \text{Alfvén velocity.}$$

Equation (89) is plotted in Figs. 13-15.

In order to obtain the necessary force for toroidal equilibrium, one sets $\delta = 0$ in Eqs. (85-87) obtaining

$$F_R = \frac{\beta B_0^2 a^2}{4R} = F_{\ell+1} = \frac{\beta}{8} B_0^2 h a^2 \delta_{\ell} \left[\frac{I'_{\ell+1}}{I_{\ell+1}} + (1 - \beta) \left(1 + \frac{\ell^2 \pm \ell}{h^2 a^2} \right) \frac{I_{\ell}}{I'_{\ell}} \right] Z_{\ell+1},$$

and using

$$\delta_{\ell+1} = \frac{M'_{\ell+1}}{h a} = \frac{1}{h a} \frac{I'_{\ell+1}}{I_{\ell+1}} Z_{\ell+1},$$

the result is

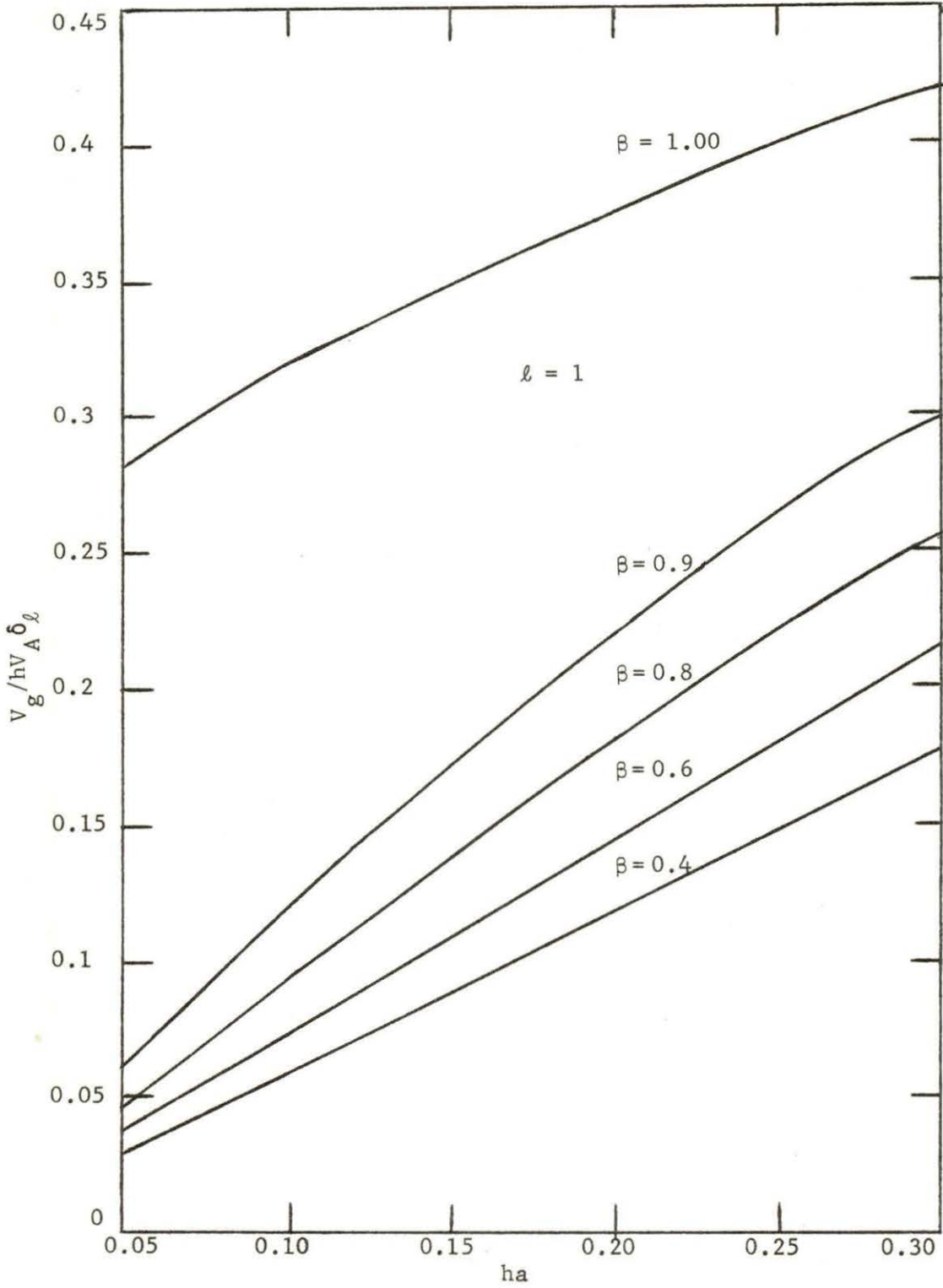


Fig. 13. Normalized growth rate versus ha for various β values and $l = 1$.

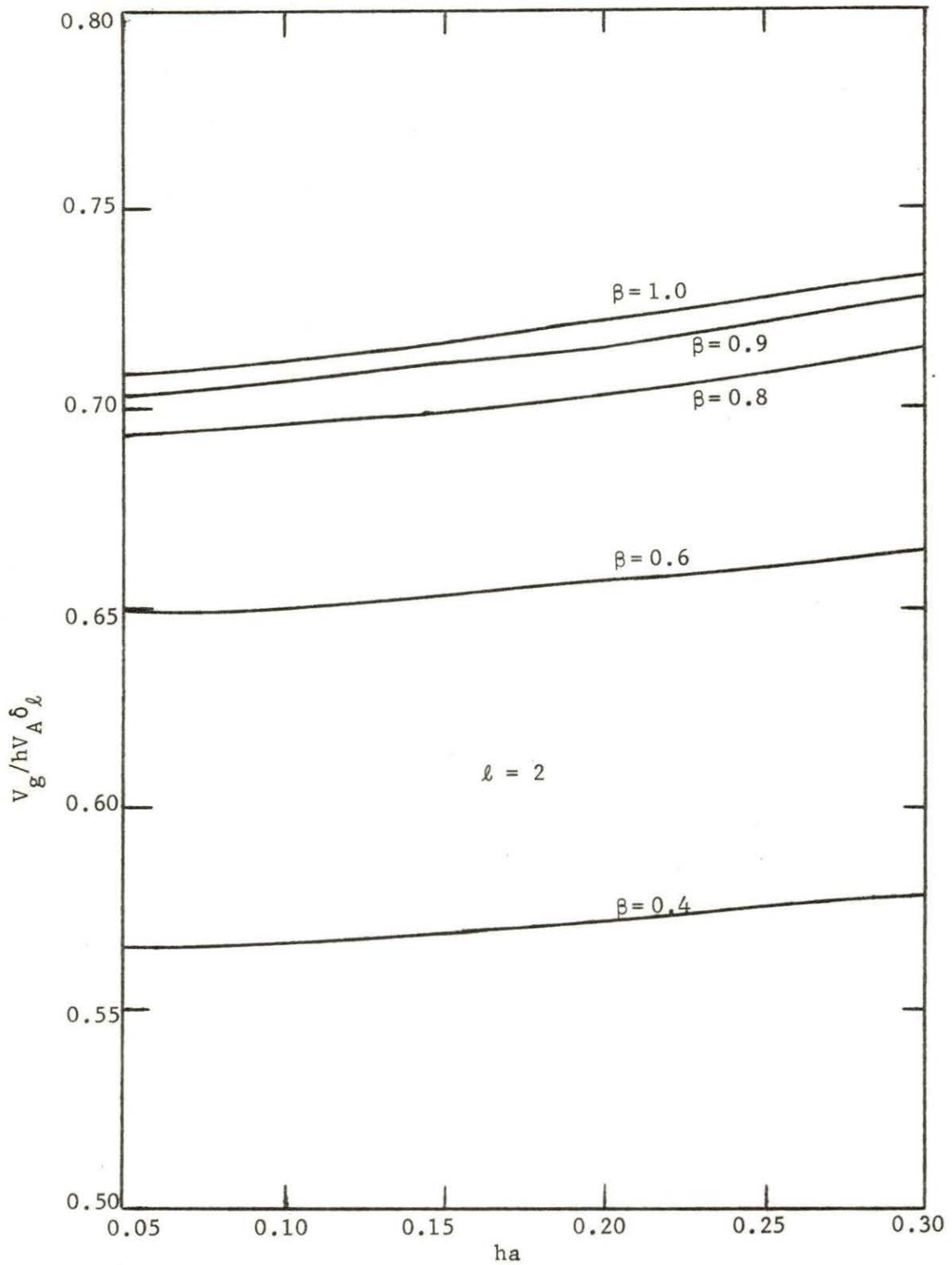


Fig. 14. Normalized growth rate versus ha for various β values and $l = 2$.

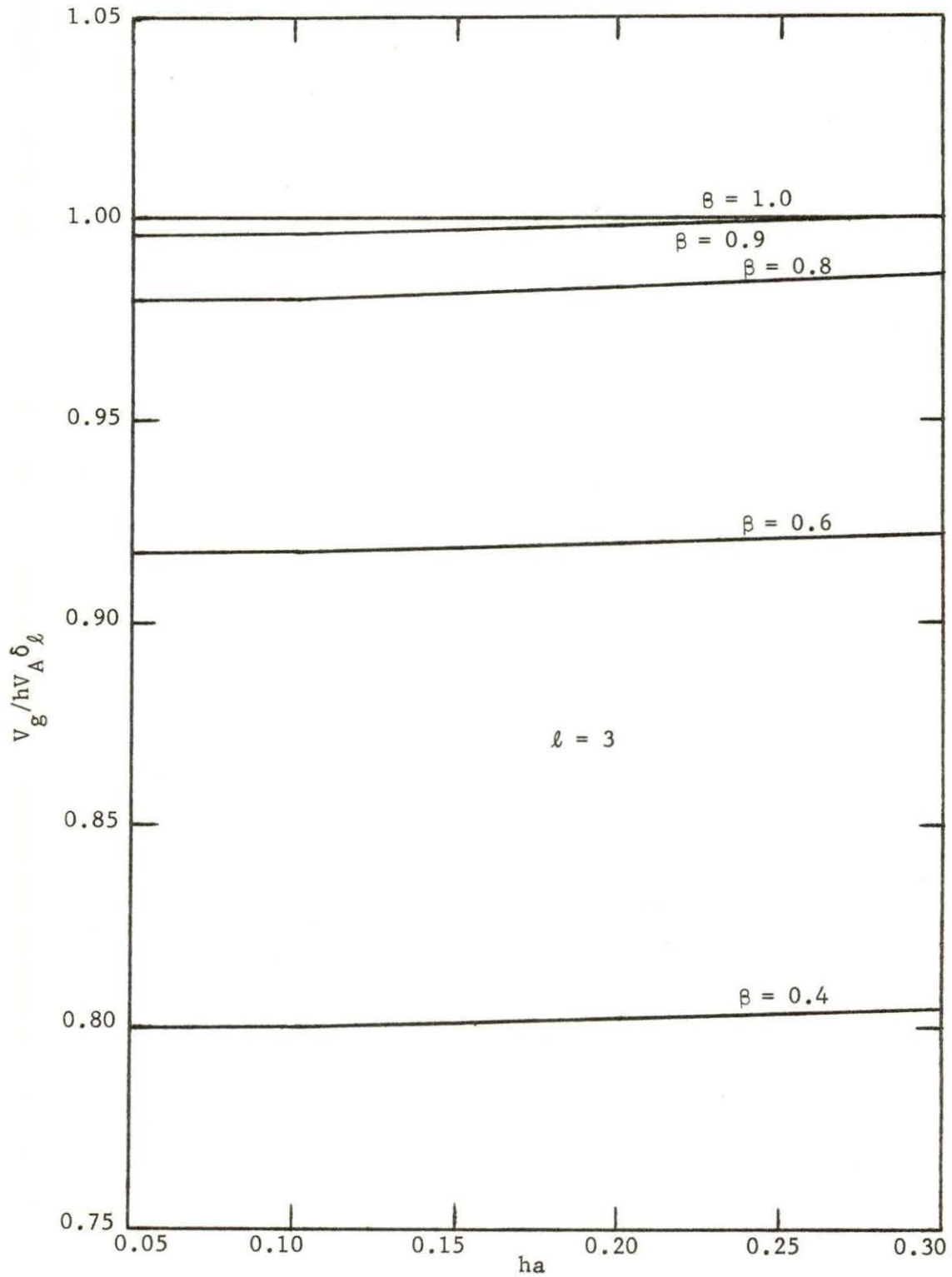


Fig. 15. Normalized growth rate versus ha for various β values and $l = 3$.

$$F_R = \frac{\beta B_o^2 a^2}{4R} = \frac{\beta}{8} B_o^2 h^2 a^3 \delta_\ell \delta_{\ell+1} \left[1 + (1 - \beta) \left(1 + \frac{\ell^2 \pm \ell}{h^2 a^2} \right) \frac{I_\ell I_{\ell+1}}{I'_\ell I'_{\ell+1}} \right]. \quad (90)$$

Equation (90) gives the balance of forces required for toroidal equilibrium.

Before comparing these analytical results with the experimental results from Scyllac [9], one must determine which magnetic fields are actually being measured. The Scyllac [9] uses $\ell = 1$ and $\ell - 1 = 0$ helical fields. For the $\ell = 1$ field, $B_r(\ell = 1)$ is being measured experimentally which allows one to directly apply Eq. (80) and Eq. (82). However, as seen on page 8 of this thesis, the measured $\ell - 1 = 0$ field will actually be $B_z(\ell - 1 = 0)$. Thus, one must use the relation

$$B_r(\ell - 1 = 0) = B_z(\ell - 1 = 0) \frac{ha}{2} \quad (91)$$

to modify Eq. (80) and Eq. (82) for use with experimentally measured $\ell - 1 = 0$ fields.

III. COMPARISON OF EXPERIMENTAL AND THEORETICAL RESULTS

An extensive number of experiments have been done on the Scyllac toroidal sector [9]. The Scyllac has a major radius of 237.5 cm and extends through an angle of 120° . The coil arc length is 5 meters, and the helical fields have one-period lengths of 33.2 cm. The toroidal sector is operated with nine variations of $\ell = 1$ and $\ell - 1 = 0$ magnetic fields to furnish toroidal equilibrium.

Equation (80) is used in the lab to calculate δ_0 and δ_1 , except for three experiments in which δ_0 is measured experimentally.

The experimental results are compared to Eq. (81) and Eq. (82) which should be satisfied for $\delta = 0$. This corresponds to an effective cancellation of the toroidal force.

Finally, Eq. (90) is used to determine if the toroidal force is effectively cancelled.

It is hoped that a correlation can be made between plasma containment time, and the agreement between theoretical and experimental values.

Each experiment will be denoted by a letter. Field configurations for each of the nine experiments is listed in Table 1.

Experiment A involved no $\ell = 1$ or $\ell - 1 = 0$ fields, but was the control experiment in a smooth-bore coil. The toroidal force caused the plasma to drift to the wall in about 2.2 μsec . The major parameters for this and all other experiments are taken for $\beta = 0.8$. At this β , the ion temperature is about 1 Kev, and the density on the axis is $2 - 3 \times 10^{16}$ particles/cm³ for a 10 m Torr deuterium filling.

Table 1. Summary of Scyllac experiments

Experiment	B_0 (KG)	$\frac{B_{\ell=0}}{B_0}$	$\frac{B_{\ell=1}}{B_0}$	δ_0	δ_1	β	a (cm)	Average coil radius (cm)
A	50	0	0	0	0	—	—	7.21
B	42.6	0.22	0.06	0.3 ^a	0.54	0.8	1.0	8.11
C	40.0	0.105	0.08	0.2 ^a	0.68	0.75	1.0	8.57
D	40.0	0.105	0.086	0.2 ^a	0.68	0.65	1.0	8.57
E	40.2	0.089	0.090	0.27	1.19	0.8	0.7	8.50
F	40.9	0.071	0.096	—	—	—	—	8.42
G	41.0	0.09	0.07	0.6	0.82	0.95	0.88	8.02
H	41.0	0.09	0.07	—	—	—	—	8.02
J	36.3	0.08	0.08	0.24	1.06	0.85	0.7	10.25

^aExperimentally measured.

Experiment B used an $\ell - 1 = 0$ groove cut into the main compression coil. The $\ell - 1 = 0$ groove depth was 1.8 cm in the main compression coil. This groove depth produced a rather large $\ell - 1 = 0$ field. The $\ell = 1$ field was produced by coils that proved to be 35% stronger in the region of the $\ell - 1 = 0$ grooves. As can be seen in Table 2, the toroidal force $F_{1,0}$ was much too large, although the containment time was double that of Experiment A.

In Experiment C the $\ell - 1 = 0$ groove depth is reduced to 0.9 cm which produced a nearly equal $\ell = 1$ field in both the land and groove region. Looking at Table 2, the $F_{1,0}$ force is too small to cancel the

Table 2. Summary of results from Scyllac

Experiment	$\left(\frac{R}{a}\right) \delta_0 \delta_1$ (Exp.)	$\left(\frac{R}{a}\right) \delta_0 \delta_1$ (Theor.)	$\left(\frac{R}{a}\right) \frac{B^0 B^1}{B_0^2}$ (Exp.)	$\left(\frac{R}{a}\right) \frac{B^0 B^1}{B_0^2}$ (Theor.)	$\frac{F_{1,0}}{F_R}$	Containment time (μsec)
B	62.9	40.0	3.13	2.0	1.58	4-6
C	30.6	37.5	1.99	2.21	0.832	6-9
D	22.6	32.5	2.14	2.84	0.694	5-7
E	80.4	81.0	2.67	2.71	0.998	12
G	132.	66.0	1.70	0.85	2.02	8
J	86.2	87.0	2.17	2.20	0.99	10

toroidal force F_R , although $F_{1,0}/F_R$ is closer to one than in Experiment B. The containment time has also greatly increased.

In Experiment D the beginning of the $\ell - 1 = 0$ fields is delayed about 0.2 μsec by means of stainless steel rings inserted into the $\ell - 1 = 0$ grooves. The general plasma motions are similar to Experiment C except the containment time is shorter. The necessary $\ell = 1$ field to achieve toroidal equilibrium was 35% more than in Experiment C. The value of current necessary for toroidal equilibrium is also much more critical when the stainless steel inserts are used.

Experiment E uses semi-cylindrical shells made of 1.5 mm thick copper in the $\ell = 0$ groove regions. These shells are made to cancel a vertical field generated on the minor axis of the torus by the applied helical fields. This is indicated theoretically by Eq. (39). These shells do an effective job of cancelling the vertical field. However,

the great increase in containment time is probably due to the satisfying of the equilibrium equations.

Experiment F used 3 mm copper shells. The values of β and a were not obtained. The behavior of the plasma is about the same as the 1.5 mm copper shell response. Using the 3 mm shells produces a containment time of only about 4-7 μsec . This is probably due to the violation of the equilibrium equations.

In Experiment G the conversion from $l = 1$ windings to $l = 1$ grooves is made. The grooving of the $l = 1$ field into the main compression coil gives a constant ratio of the $l = 1$ field to the main compression with time. It is also hoped that this groove design will simplify the production of the $l = 0, 1$ configuration. This field is produced by eight discrete sections of wavelength 33.2 cm.

The above configuration produced discharges that are more reproducible from discharge to discharge than if the $l = 1$ winding is used.

In Experiment H the grooved $l - 1 = 0$ and $l = 1$ compression coil is used. In this case the equilibrium equations were satisfied, and a containment time of 12 μsec was reached. The superposition of a 600 G vertical field of either polarity had little effect on the containment time.

In Experiment J the grooved compression coil is designed to produce very accurate $l - 1 = 0$ and $l = 1$ fields. Each wavelength is divided into 260 steps which should provide an improvement over the double-grooved coil in Experiments G and H.

Plasma equilibrium is obtained by adjusting the initial deuterium filling pressure in order to satisfy the equilibrium equations for their β dependence. The satisfying of the theoretical equilibrium equations results in a rather high containment time as shown in Table 2.

A superimposed vertical field can be varied from - 430 to 700 G with little change in plasma behavior.

Figures 16 and 17 are derived from Table 2, Fig. 5, and Fig. 9. It is also necessary to use Eq. (91). These plots indicate that only Experiments E and J satisfy the theoretical conditions for plasma equilibrium.

It was noted before that δ_0 was experimentally measured from luminosity profiles for Experiments B, C, and D. Figure 18 compares these measured values with the expected theoretical values taken from Fig. 1 where Eq. (91) must be used once again. As seen in Table 1 these values of δ_0 are only accurate to one significant figure. Thus, one cannot infer too much from Fig. 18.

It was assumed throughout the rest of the experiments that δ_0 and δ_1 would be more accurate if calculated from Eq. (80) rather than measured experimentally.

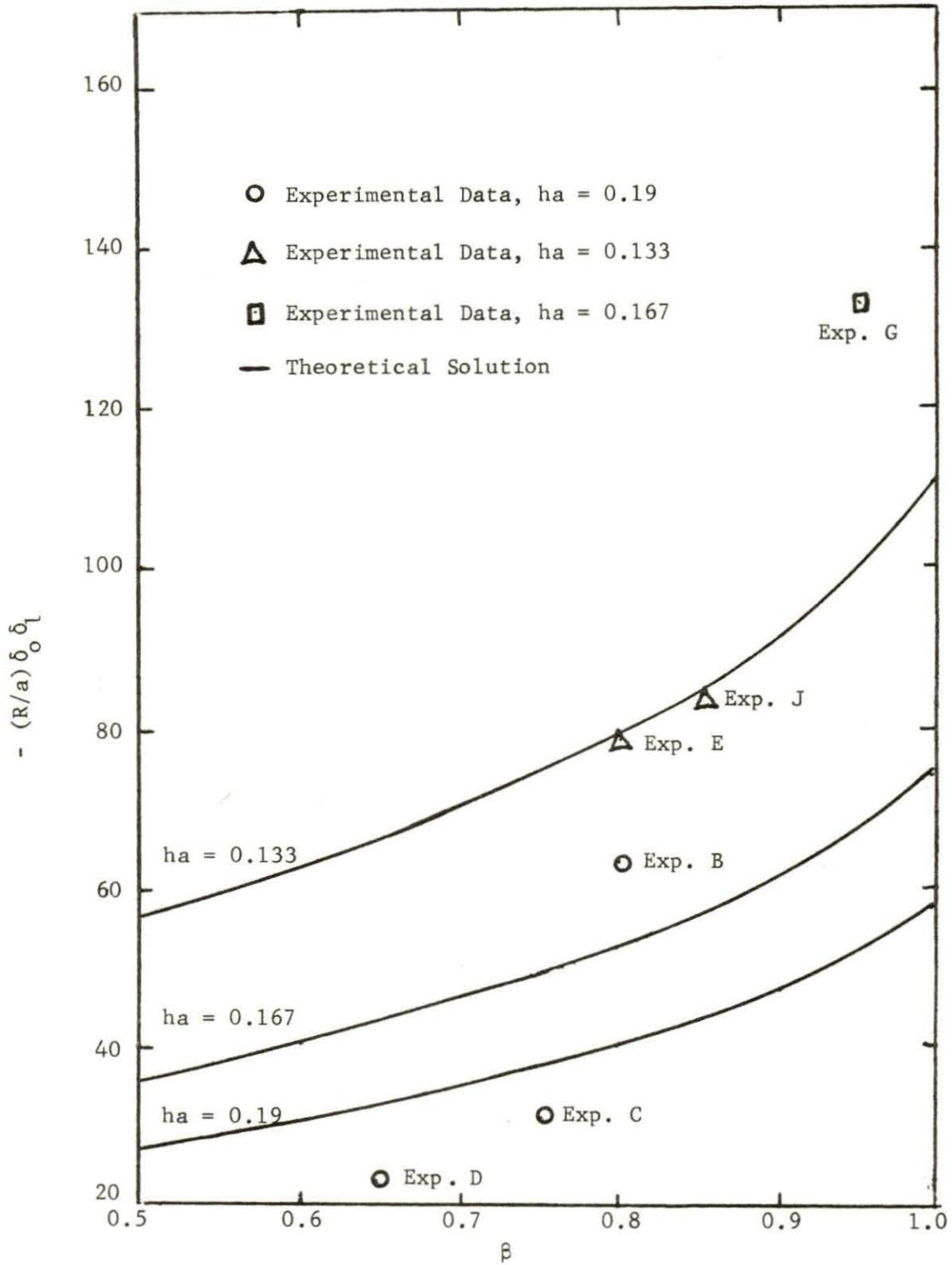


Fig. 16. The quantity $-(R/a) \delta_0 \delta_1$ versus β for experimental trials and theoretical solution.

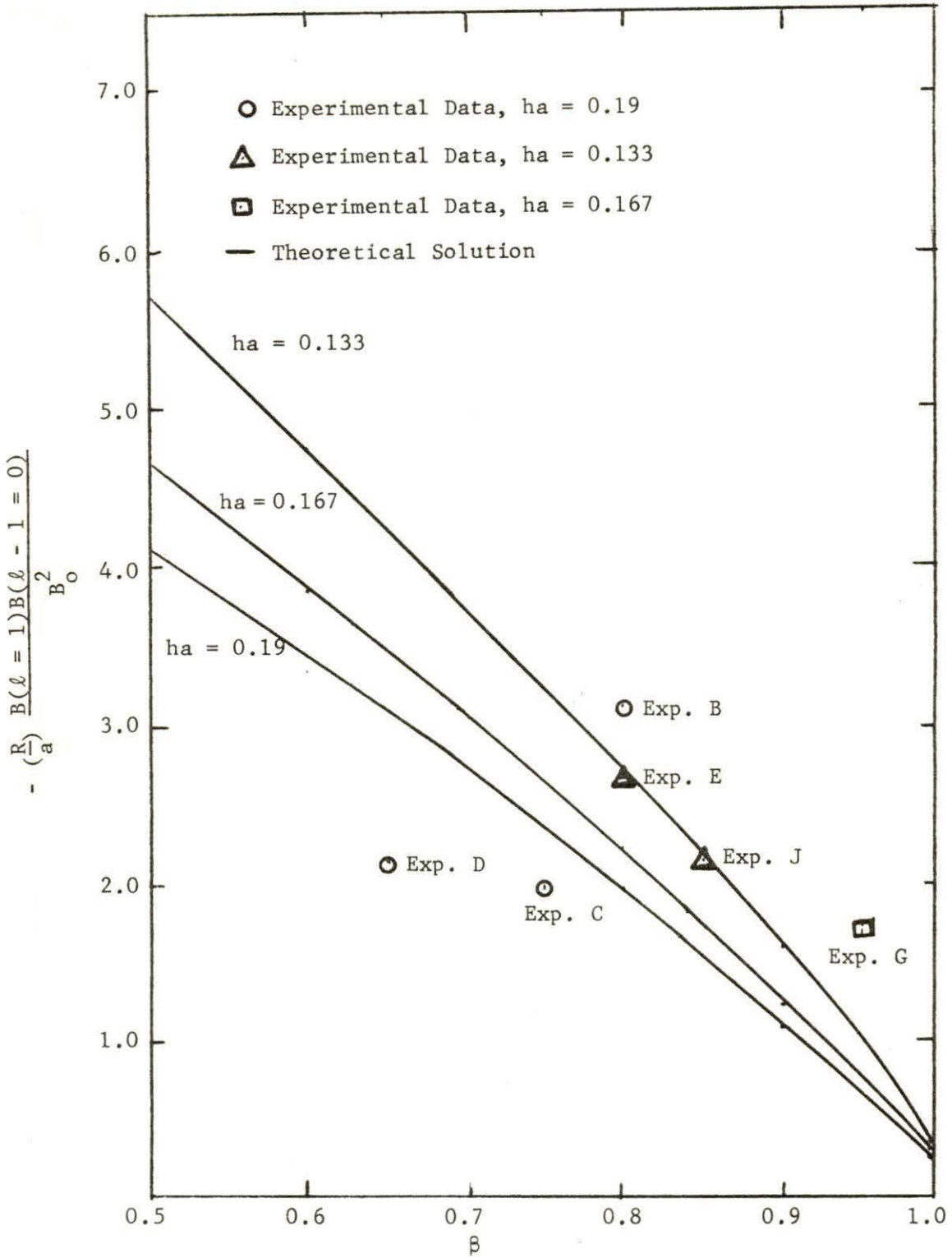


Fig. 17. The quantity $-\left(\frac{R}{a}\right) \frac{B(\ell = 1)B(\ell - 1 = 0)}{B_0^2}$ versus β for experimental trials and theoretical solution.

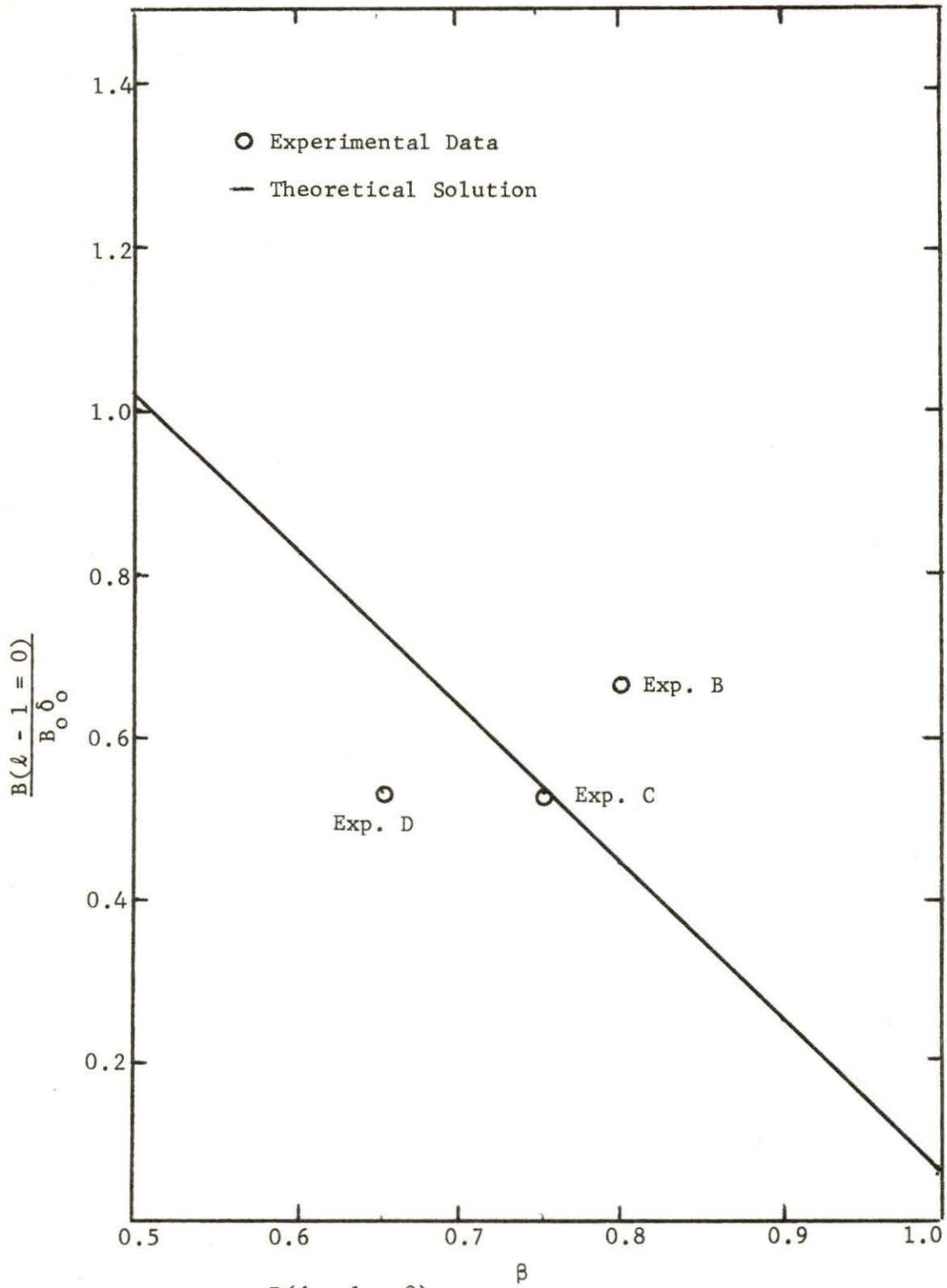


Fig. 18. The quantity $\frac{B(\ell - 1 = 0)}{B_0 \delta_0}$ versus β for $ha = 0.19$.

IV. DISCUSSION AND CONCLUSIONS

In the present ordering δ_ℓ and $\delta_{\ell+1}$ are considered zero-order and first-order, respectively. While the old ordering done by Ribe [7, 10] considers δ_ℓ and $\delta_{\ell+1}$ as first- and second-order quantities. Taking δ_ℓ as a zero-order quantity created many problems when using the many Taylor series expansions. It allowed for the creation of so many new terms that the entire problem became insolvable. Thus, the assumption made for the present expansion involved the ignoring of terms multiplied by the square of an ℓ -order field. According to current experimentation, the assumption seems to be a rather good one.

Ribe [7, 10] also considered h_a to be a zero-order quantity, while in the present expansion h_a is taken as a first-order quantity. It has been seen in the derivation that the use of h_a as a first-order quantity has important consequences. The magnitude of many of the fields are changed, and $M_{\ell-1} = M_0$ must be treated as a special case.

Thus, the present ordering drastically changes the expansion calculations. However, the final result is the same as that derived by Ribe [7, 10] using the old ordering. The present expansion greatly extends the region over which the equations are applicable. The equations should be accurate for present experiments where h_a is taken as a first-order quantity.

If the toroidal drift is to be effectively cancelled, the experimental and theoretical values of $(R/a)\delta_1\delta_0$ and $(R/a)B_{\ell=1}B_{\ell=0}/B_0^2$ should be equal, and the expression $F_{1,0}/F_R$ should equal one.

The general conclusions drawn from Table 2 is that when the theoretical equations are satisfied, (as stated above) the containment time is much longer than when they are not. This can be seen from Experiments E and J in Table 2. Even though each experiment uses different coil configurations, the most important factor concerning containment time is that the theoretical equations are satisfied.

Thus, stuffing the $\ell = 0$ grooves with stainless steel inserts, to delay the $\ell = 0$ field $0.2 \mu\text{sec}$, has little effect on containment time. In fact, a 35% increase in the $\ell = 1$ field is necessary in order to give toroidal equilibrium.

The replacing of the $\ell = 1$ winding with the grooved $\ell = 1$ coil seemed to improve time and spatial uniformity of the $\ell = 1$ field. However, the general plasma motion in the grooved case is not much different from the plasma motion obtained while using $\ell = 1$ windings.

It is noted that a transverse field varying in magnitude from - 430 to 770 G can be superimposed on the helical fields with little change in plasma motion. However, it is concluded that this may be due to end effects of the 5-meter device. The vertical fields may have more of an effect when the full torus is used.

These experiments have certainly demonstrated the usage of the $\ell = 1, 0$ toroidal equilibrium. They have also indicated the good agreement between experimental plasma equilibrium and theoretical equilibrium predicted by the present expansion using sharp-boundary MHD theory.

The plasma containment time has been increased to as high as $12 \mu\text{sec}$ using $\ell = 1, 0$ fields. At this time an $m = 1$ motion drives

the plasma toward the wall. This may be due to the long wavelength $m = 1$ instability or an imbalance between $F_{1,0}$ and F_R as the plasma parameters vary with time.

Further experiments on the Scyllac will best be done on a full torus in which end effects can be avoided.

V. TOPICS FOR FURTHER STUDY

It may be possible to improve the solution by including more terms in the Taylor series expansions and then using numerical techniques to obtain a solution.

The sharp boundary model may be somewhat questionable. Another simple model may be tried that approximated a diffuse boundary. However, the complexity of the problem may become too great.

The greatest need for further study lies in the area of experimentation. Experiments on a completed torus could answer many questions.

VI. LITERATURE CITED

1. A. A. Blank, H. Grad, and H. Weitzner in "Plasma Physics and Controlled Nuclear Fusion Research," IAEA, Vienna, March 1969, vol. 2, pp. 607-617.
2. J. P. Freidberg, Physics of Fluids, 14, 2454 (1971).
3. H. Grad and H. Weitzner, Physics of Fluids, 12, 1725 (1969).
4. J. M. Greene, J. L. Johnson, and K. E. Weimer, Plasma Physics, 12, 145 (1965).
5. A. I. Morozov and L. S. Solovev, Reviews of Plasma Physics, 2, 42 (1966).
6. R. L. Morse, W. B. Riesenfeld, and J. L. Johnson, Plasma Physics, 10, 543 (1967).
7. F. L. Ribe, "Free Boundary Solutions for High-Beta Stellarators of Large Aspect Ratio," LA-4098, Los Alamos Scientific Laboratory, 1969.
8. F. L. Ribe, "Progress Report of the LASL Controlled Thermonuclear Research Program for a 12-Month Period Ending October 1971," LA-4888-PR, Los Alamos Scientific Laboratory, 1971.
9. F. L. Ribe, "Progress Report of the LASL Controlled Thermonuclear Research Program for a 12-Month Period Ending December 1972," LA-5250-PR, Los Alamos Scientific Laboratory, 1972.
10. F. L. Ribe and M. N. Rosenbluth, Physics of Fluids, 13, 2572 (1970).
11. M. N. Rosenbluth, J. L. Johnson, J. M. Greene, and K. E. Weimer, Physics of Fluids, 12, 726 (1969).
12. K. S. Thomas, C. R. Harder, W. E. Quinn, and R. E. Siemon, Physics of Fluids, 15, 1658 (1972).
13. H. Weitzner, Physics of Fluids, 14, 658 (1971).

VII. ACKNOWLEDGMENTS

The author wishes to express his gratitude to Dr. B. M. Ma of the Department of Nuclear Engineering for his many helpful suggestions during this study. Also, thanks go to the Air Force for their support of an assistantship under which this work was accomplished.

The author wishes to express his gratitude to his wife, Mary Jane, for her encouragement and help in preparing the manuscript.